# Dense shelf-water and associated sediment transport in the Cap de Creus Canyon and adjacent shelf under mild winter regimes: insights from the 2021-2022 winter

- 4 Marta Arjona-Camas <sup>1,2,\*</sup>, Xavier Durrieu de Madron<sup>2</sup>, François Bourrin<sup>2</sup>, Helena Fos<sup>1</sup>, Anna Sanchez-
- 5 Vidal<sup>1</sup>, David Amblas<sup>1</sup>

1

2

3

9

10

11

12

13

14 15

16

17

18

19

20

21

22

23

24

25

26

27

28

29

30

31 32

33

34

35

36

37

38

39

40

41

- 6 ¹GRC Geociències Marines, Departament de Dinàmica de la Terra i de l'Oceà, Universitat de Barcelona, Barcelona, Spain.
- 7 <sup>2</sup>CEFREM, UMR-5110 CNRS-Université de Perpignan Via Domitia, Perpignan, France.
- 8 *Correspondence to*: Marta Arjona-Camas (marjona@ub.edu)

Abstract. Dense shelf water cascading (DSWC) is a key oceanographic process in transferring energy and matter from continental shelves to deep ocean areas. Although intense DSWC (IDSWC) events have received most attention due to their large impacts, mild DSWC (MDSWC) events are the most frequent in the northwestern Mediterranean and are expected to become more common under climate change. However, their dynamics, particularly in the Cap de Creus Canyon, have been less comprehensively described and compared to strong-winter events. This study investigates MDSWC in the Cap de Creus Canyon during the mild winter of 2021-2022, examining shelf-canyon transports of both dense shelf waters and suspended particulate matter (SPM). Observations from the FARDWO-CCC1 multiplatform cruise in March 2022 revealed the presence of cold, dense, and turbid -shelf waters, enriched in dissolved oxygen and chlorophyll-a, on the continental shelf adjacent to the canyon. These waters, which cascaded into the canyon head and progressed further into the canyon along its southern flank to ~390 m depth., yet its dynamics under mild winter regimes remain poorly characterized. This study investigates shelf-slope transports of dense shelf waters and suspended particulate matter in the Cap de Creus Canyon (northwestern Mediterranean) during the mild winter of 2021-2022. Observations from the FARDWO-CCC1 multiplatform cruise in March 2022 revealed the presence of dense shelf waters on the continental shelf, which were transported to the canyon head. These cold, dense, and turbid waters, rich in dissolved oxygen and chlorophyll a, downwelled along the canyon's southern flank to ~390 m depth. Estimated water and SPM suspended sediment transports during this event were 0.7 Sv and 10<sup>5</sup> metric tons (t), respectively, at the continental shelf. Within the canyon, transports were 0.3 Sy and 10<sup>5</sup> metric tonst, respectively, mainly confined to in the upper canyonsection, while m. Mid-canyon transports were lower (0.05 Sv and 10<sup>4</sup>t, respectively), indicating that most dense shelf waters likely remained confined to the shelf area and upper canyon. During this event, dense shelf waters were transported ~30 km from the shelf into the canyon. Our results show that significant transport of dense shelf waters (260 km<sup>3</sup>) and suspended sediment can occur in the Cap de Creus Canyon during MDSWC events under mild winters, also contributing significantly to the formation of Western Intermediate Water (WIW) in the canyon. The Mediterranean Sea Physics reanalysis data indicate that the cascading season lasted from late-January to mid-March 2022, with several shallow cascading pulses throughout this period. Peak transport , poccurred ineaking in mid-March associated with during an eastern storman easterly/southeasterly storm, .suggestingwhich likely intensified MDSWC in the canyon. Our study reinforces the idea that dense shelf water transports exhibit marked interannual variability, even under mild winters. that during mild winters, dense waters either remain on the shelf, flow along the coast, or cascade only to the upper section of the Cap de Creus Canyon. Our results show that significant export of dense shelf water (260 km<sup>3</sup>) and suspended sediment can occur in the Cap de Creus Canyon under more moderate atmospheric forcings and shallow cascading. The Mediterranean Sea Physics reanalysis data indicate that the cascading season lasted from late-January to mid-March 2022, with several shallow cascading pulses, peaking in mid-March during an easterly/southeasterly storm. Our results show that significant export of dense shelf water (260 km³) and suspended sediment can occur in the Cap de Creus Canyon under more moderate atmospheric forcings and shallow easeading. Nevertheless, mild DSWC events likely make a significant contribution to the Western Intermediate Water (WIW) body in the canyon.

**Keywords:** dense shelf water cascading; Western Intermediate Water; mild winter; sediment transport; reanalysis; Gulf of Lion; Mediterranean Sea.

#### 1. Introduction

Continental margins are dynamic transition zones that connect the terrestrial and ocean systems, and play a key role in the transfer and redistribution of particulate material (Nittrouer et al., 2009; Levin and Sibuet, 2012). These regions often receive substantial inputs of sediment, especially from rivers and atmospheric deposition (Blair and Aller, 2012; Liu et al., 2016; Kwon et al., 2021). While much of this material accumulates on the continental shelf, various hydrodynamic processes, such as storm waves, river floods, or ocean currents, can resuspend and transport sediments towards the continental slope and deeper areas of the ocean (Walsh and Nittrouer, 2009; Puig et al., 2014).

One particularly efficient mechanism of shelf-to-slope exchanges is dense shelf water cascading (DSWC). DSWC is a seasonal oceanographic phenomenon that occurs in marine regions worldwide. DSWC starts when surface waters over the continental shelf become denser than surrounding waters by cooling, evaporation, or sea-ice formation with brine rejection (e.g., Ivanov et al., 2004; Durrieu de Madron et al., 2005; Canals et al., 2006; Amblas and Dowdeswell, 2018; Mahjabin et al., 2019, 2020; Gales et al., 2021). Dense shelf waters then sink, generating near-bottom gravity flows that move downslope, frequently funneled through submarine canyons (Allen and Durrieu de Madron, 2009). This process contributes to the ventilation of the deep ocean, and plays an important role in the global thermohaline circulation. Additionally, it modifies the seabed along its path by eroding and depositing sediments, and facilitates the transfer of energy and matter (including sediment particles, organic carbon, pollutants, and litter) from shallow to deep waters (Canals et al., 2006; Tubau et al., 2013; Puig, 2017; Amblas and Dowdeswell, 2018).

The Gulf of Lion (GoL), located in the northwestern Mediterranean, is a very interesting region to study DSWC and shelf-slope exchanges. This region receives important inputs from riverine discharge and atmospheric deposition, and is subject to intense physical forcing (Durrieu de Madron et al., 2008). Episodic events, such as storms or DSWC, efficiently contribute to the export of shelf waters and sediments towards the open sea and deeper parts of the basin (Millot, 1990; Canals et al., 2006; Palanques et al., 2006, 2008; Ogston et al., 2008). The formation of dense waters in the GoL essentially occurs in winter, triggered by persistent (> 30 consecutive days) northerly and north-westerly winds (locally named Tramontane and Mistral) that induce surface heat loss, evaporation, vertical mixing, and the subsequent densification of shelf waters (Durrieu de Madron et al., 2005, 2008; Canals et al., 2006; Durrieu de Madron et al., 2013). These dense waters sink until reaching their equilibrium depth and propagate along the western coast of the GoL (Fig. 1). The combined effect of the prevailing cyclonic coastal circulation and the narrowing of the continental shelf near the Cap de Creus Peninsula (Fig. 1), concentrates most of this dense water at the southwestern end of the GoL, where it is mainly exported through the Lacaze-Duthiers and Cap de Creus canyons (Ulses et al., 2008b; Palanques et al., 2008). In these canyons, dense waters overspill the shelf edge and cascade down the slope (Béthoux et al., 2002; Durrieu de Madron et al., 2005), contributing to the ventilation of intermediate and deep layers. As they descend, these overflows reshape the seabed by eroding and depositing sediments, and promote the downslope transport of organic matter accumulated on the shelf. Ultimately, DSWC in the GoL has been observed to impact biogeochemical cycles and the functioning of deep-sea ecosystems (Bourrin et al., 2006, 2008; Heussner et al., 2006; Sanchez-Vidal et al., 2008).

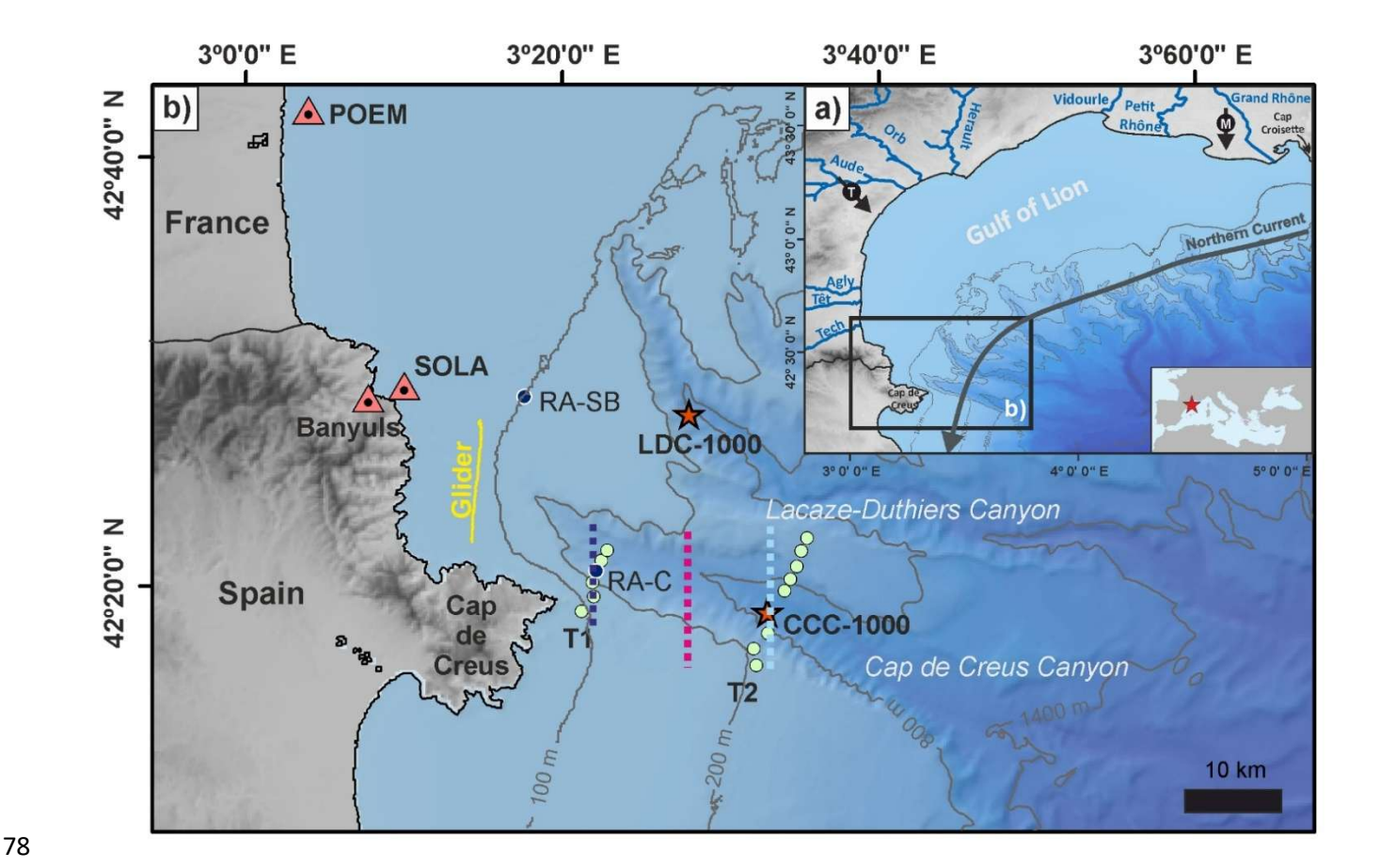


Figure 1. (a) Bathymetric map of the GoL showing the rivers discharging into the gulf and the incised submarine canyons. Black arrows depict Tramontane and Mistral winds. The grey arrow indicates the direction of the Northern Current over the study area. (b) Bathymetric map of the southwestern part of the Gulf of Lion showing the location of Lacaze-Duthiers Canyon (LDC) and Cap de Creus Canyon (CCC). Orange triangles indicate the location of buoys (POEM, Banyuls, and SOLA). The location of the re-analysis grid-points at the shelf break (RA-SB) and within the CCC (RA-C) are indicated with dark blue dots. Green dots represent the location of CTD stations carried out during the FARDWO-CCC1 cruise. Red stars mark the location of two instrumented mooring lines deployed at ~1000 m depth at the axis of LDC (LDC-1000) and CCC (CCC-1000). The solid yellow line indicates the glider section on the continental shelf adjacent to the CCC. Dashed lines correspond to the virtual transects defined using reanalysis data: dark blue and light blue lines indicate the location of the upper and mid-canyon transects, respectively, used to estimate dense water transport during winter 2021-2022; the fuchsia dashed line marks the central canyon transect used to determine the temporal evolution of cascading events over the past 26 years (1997-2022).

Due to its relative ease of access, the GoL is particularly suitable for investigating DSWC. However, because of its intermittent nature, DSWC remains difficult to observe directly and its contribution to shelf-deep-slope ocean-exchanges is challenging to quantify. Several studies in the GoL have focused on the impact of intense DSWC (IDSWC) events on shelf-slope exchanges. These particularly extreme events were monitored in the winters of 1998-1999 (Heussner et al., 2006), 2004-2005 (Canals et al., 2006; Ogston et al., 2008; Puig et al., 2008), 2005-2006 (Pasqual et al., 2010; Sanchez-Vidal et al., 2008; Pasqual et al., 2010), and 2011-2012 (Durrieu de Madron et al., 2013; Palanques and Puig, 2018), with instrumented mooring lines deployed at ~1000 m depth in Lacaze-Duthiers and Cap de Creus Canyons. One of the most studied IDSWC events occurred in the severe winter of 2004-2005, when Over over 40 days, more than two thirds (750 km³) of GoL's shelf waters cascaded through the Cap de Creus Canyon (Canals et al., 2006; Ulses et al., 2008b), 1. This event was characterized bymaintaining cold temperatures (11-12.7 °C), high densities (σθ ≥ 29.1 kg·m⁻³), high strong down-canyon velocities (> 0.8

m·s<sup>-1</sup>), and high suspended sediment concentrations (30-40 mg·L<sup>-1</sup>), and transported . This DSWC event also transported  $\sim 0.6 \cdot 10^6$  tons of organic carbon downcanyon, a mass comparable to the mean annual solid transport of all rivers discharging into the GoL (Canals et al., 2006; Tesi et al., 2010).

101

102

103

104

105

106

107

108

109

110

111

112

113

114

115

116

117

118

119

120

121

L22

123

124

L25

L26 L27

28

L29

.30

131 132

L33

L34

L35

.36

L37

L38

L39

140

141

Although IDSWC events have drawn particular attention due to their significant impacts, mild or shallow DSWC (MDSWC) events are in fact the most frequent since the set of the observational era in the GoL, and they are expected to become more prevalent under the climate change scenario (Herrmann et al., 2008; Durrieu de Madron et al., 2023). These events typically occur during mild winters, characterized by quieter atmospheric conditions and lower heat losses (Martín et al., 2013; Rumín-Caparrós et al., 2013; Mikolajczak et al., 2020). During such winters, the cold continental winds that drive dense water formation are weaker and less persistent, typically blowing for fewer than 30 days and rarely exceeding speeds of 10 m·s<sup>-1</sup>. In contrast, easterly and southeasterly winds become unusually more frequent and sustained, sometimes blowing for more than three consecutive days (Ferré et al., 20052008). They do not produce a densification of surface waters but lead to an intense cyclonic circulation on the GoL's shelf (Ulses et al., 2008a; Mikolajczak et al., 2020). At the same time, river discharges, particularly from the Rhône River, supply freshwater to the GoL's shelf, further limiting locally the densification of shelf waters (Ulses et al., 2008a). The cyclonic circulation on the shelf can promote the accumulation of light shelf waters  $(\sigma\theta \approx 27.78 \text{ kg} \cdot \text{m}^{-3})$  along the coast and their subsequent downwelling into the Cap de Creus Canyon, without cascading offshelf (Martín et al., 2013; Rumín-Caparrós et al., 2013). Under mild winter conditions, shelf waters can continue to gain density on the shelf, reaching  $\sigma\theta \approx 28.9-29.1~{\rm kg\cdot m^{-3}}$  and cascading typically to depths ~400 m depth into the canyon. This shallow cascading allows dense shelf waters to descent just above the intermediate-water layer, where they contribute to the formation of Western Intermediate Water (WIW) (Dufau-Julliand et al., 2004; Herrman et al., 2008).

The mechanisms driving MDSWC events during mild winters are relatively well described, but their magnitude and contribution to shelf-to-slope exchanges remain less quantified. Previous studies have provided first-order estimates of dense water transports during MDSWC events. For instance, At the same time, river discharges, particularly from the Rhône River, supply freshwater to the GoL's shelf, further limiting the densification of shelf waters (Ulses et al., 2008a). As a result, most of the dense shelf waters are mixed with lighter ambient waters on the shelf before reaching the slope, and only a small fraction is exported along the coast or to the upper slope, where it contributes to the body of Western Intermediate Water (Duffau-Juliand et al., 2004; Herrmann et al., 2008). Ulses et al. (2008a) estimated a total export transport of dense shelf waters of 75 km³ in the mild winter of 2003-2004, an order of magnitude smaller than during IDSWC events. Similarly, during the winter of 2010-2011, only brief and shallow cascading was observed in the Cap de Creus Canyon down to 350 m depth (Martín et al., 2013; Rumín Caparrós et al., 2013). More recently, modeling studies have expanded our understanding on the interannual variability of dense water export transports under different atmospheric scenarios, and emphasized the role of moderate mild winters in driving MDSWC events in the GoL (Mikolajczak et al., 2020).

-Nonetheless, most existing existing studies have relied on numerical simulations and or time series from fixed mooring stations, which offer limited spatial and temporal resolution and lack do not fully capture direct observations of shelf-to-slope exchanges. Consequently, there is still a lack of direct observational evidence documenting the transport of dense shelf waters and suspended particulate matter (SPM) from the shelf to the canyon under mild winter conditions, as well as how these events compare to the full spectrum of cascading events observed in the Cap de Creus Canyon. To date, there has been no comprehensive observational characterization of dense water and sediment transport from the shelf to the slope in the Cap de Creus Canyon under moderate winter conditions during MDSWC events. To address this gap, the present study documents and characterizes a MDSWC event in the Cap de Creus during the mild winter of 2021-2022. We combine hydrographic and velocity measurements collected within the canyon and on the adjacent shelf to investigate the shelf-to-slope-canyon transports

of dense waters and suspended sediment, along with reanalysis data to determine the temporal extent of this event and place it in the broader context in the context of cascading events observed in the Cap de Creus Canyon over the past 26 years. By focusing on a mild winter scenario, we aim to provide insights into MDSWC events and discuss the implications for WIW formation and deep-sea ecosystems.

#### 2. Study area

#### 2.1. General setting

The GoL is a micro-tidal river-dominated continental margin that extends from the Cap Croisette Peninsula, in the northern part of the gulf, to the Cap de Creus Peninsula at its southwestern limit (Fig. 1a). It is characterized by a wide continental shelf (up to 70 km) and it is incised by a dense network of submarine canyons (Lastras et al., 2007).

The GoL is impacted by strong continental winds from the north and northwest (Mistral and Tramontane, respectively), which favor dense water formation and cascading events in winter (Durrieu de Madron et al., 2013) and coastal upwellings in summer (Odic et al., 2022). Humid easterly and southeasterly winds, which blow less frequently, occur primarily from autumn to spring, and can produce large swells and high waves over the continental shelf (Ferré et al., 20085; Leredde et al., 2007; Petrenko et al., 2008; Guizien, 2009). They do not produce a densification of surface waters but <u>-they</u> lead to an intense cyclonic circulation on the GoL's shelf and to a strong export of shelf waters at the southwestern exit of the GoL (Ulses et al., 2008a; Mikolajczak et al., 2020).

The ocean circulation of the GoL is also influenced by the freshwater inputs from the Rhône River, one of the largest Mediterranean Rivers, and a series of smaller rivers with typical flash-flooding regimes (Ludwig et al., 2009). The Rhône River supplies an annual river discharge of 1700 m³·s⁻¹ and an average of 8.4 Mt·y¹ of suspended particulate matter (Sadaoui et al., 2016; Poulier et al., 2019). The smaller rivers (from south to north the Tech, Têt, Agly, Aude, Orb, Hérault, Lez, and Vidourle) account for slightly 5% of the total inputs of particulate matter (~0.5 Mt·y⁻¹) to the GoL (Serrat et al., 2001; Bourrin et al., 2006). Most of the sediment delivered by these rivers is temporarily stored near their mouths in deltas and prodeltas (Drexler and Nittrouer, 2008), and afterwards it is remobilized and redistributed along the margin by the action of storms and wind-driven along-shelf currents (Estournel et al., 2023). These coastal currents is westerly current carry ies particulate material from the shelf towards the southwestern end of the GoL, where the continental shelf rapidly narrows and the Cap de Creus Peninsula constraints the circulation, intensifying the water flow and increasing the particle concentration (Durrieu de Madron et al., 1990; Canals et al., 2006).

The Cap de Creus Canyon represents the limit between the GoL and the Catalan margin (Fig. 1b). The canyon head is located only 4 km from the coast and incises the shelf edge at 110-130 m depth (Lastras et al., 2007). Due to its proximity to the coast and the preferential direction of coastal currents, this canyon has been identified as the main pathway for the transfer of water and sediments from the shelf to the slope and deep margin (Canals et al., 2006; Palanques et al., 2006, 2012).

#### 2.2. Hydrography

The surface layers over the GoL shelf stratify between late spring and autumn (Millot, 1990). In winter, surface cooling and wind-driven mixing weaken the stratification, which leads to a vertically homogeneous water column over the continental shelf (Durrieu de Madron and Panouse, 1996). Offshore, the GoL is characterized by several water masses. The Atlantic Water (AW) fills the upper 250 m and flows into the Mediterranean Sea through the Strait of Gibraltar. During its transit to the GoL, its hydrographic properties undergo chemical and physical modifications, becoming the "old" Atlantic Water (oAW) with T > 13 °C and S = 38.0-38.2 (Millot, 1999). Below, the Eastern Intermediate Water (EIW) occupies the water column between 250 and 850 m depth. It is formed during winter in the Levantine Basin, in the Eastern Mediterranean Sea, by intermediate convection (Font, 1987; Millot, 1999; Taillandier et al., 2022; Schroeder et al., 2024). The Western

Mediterranean Deep Water (WMDW) occupies the deepest bathymetric levels and is formed in winter at interannual scales in the GoL by open-ocean deep convection. It typically shows T ~ 13 °C and S = 38.43-38.47 (Marshall and Schott, 1999; Somot et al., 2016). During winter, northerly and north-westerly winds cause the formation of dense shelf waters (DSW) over the GoL's shelf (T < 13 °C and S < 38.4) (Houpert et al., 2016; Testor et al., 2018). During mild winters, these dense waters do not gain enough density ( $\sigma$  < 29.105 kg·m<sup>-3</sup>) to sink into the deep basin, and contribute to the Western Intermediate Water (WIW) (T = 12.6-13.0 °C and S = 38.1-38.3) body found at upper slope depths (~380-400 m) (Dufau-Julliand et al., 2004; Durrieu de Madron et al., 2005; Juza et al., 2013). The formation of WIW is an important process in the Mediterranean Thermohaline Circulation (MTHC), as it contributes to the ventilation of intermediate layers and plays a role in preconditioning the region for deeper convection events (Juza et al., 2019). During extreme winters, the potential density of DSW exceeds that of the EIW ( $\sigma$  = 29.05-29.10 kg·m<sup>-3</sup>) and even surpasses the density of the WMDW ( $\sigma$  = 29.10–29.16 kg/m<sup>3</sup>), enabling DSWC to reach the deep basin around 2000-2500 m depth. This process contributes to the ventilation of the deep waters and to the final characteristics of the WMDW (Durrieu de Madron, 2013; Palanques and Puig, 2018).

#### 3. Materials and methods

#### 3.1. Field data

#### 3.1.1. Hydrographic transects and current vertical profiles

During the FARDWO-CCC1 Cruise, onboard the R/V *Garcia del Cid*, two hydrographic transects were conducted on March 5-6, 2022, across the Cap de Creus Canyon, with stations spaced every 1.5 km (Fig. 1b). The T1 transect covered the upper section of the canyon, while the T2 transect covered the mid-canyon section (Fig. 1b). The hydrographic data were collected using a SeaBird 9 CTD probe coupled with a SeaPoint Fluorometer and Turbidity Sensor (700 nm), an SBE43 dissolved oxygen sensor, and a WetLabs C-Star Transmissometer (650 nm). These sensors were mounted on a rosette system with twelve 12 L Niskin bottles, which collected water samples from various depths. The CTD-Rosette system was hauled through the water column, allowing the comparison of sensor outputs in productive surface waters with high fluorescence, in clear mid-waters, and in intermediate and bottom nepheloid layers loaded with fine suspended particulate matterparticles. The hydrographic profiles obtained from the CTD stations were interpolated onto a regular grid using the isopycnic gridding method integrated in the Data-Interpolating Variational Analysis (DIVA) gridding software from Ocean Data View (ODV) (v.5.7.2) (Schlitzer, 2023). This method is an advance gridding procedure that aligns property contours along lines of constant potential density (isopycnals) rather than constant depth, which improves the representation of water mass structure and reduces artificial smoothing across density gradients (Schlitzer, 20222023). For the interpolation, scale lengths were set to 200 m horizontally and 1 m vertically, with a quality limit of 3.0 and excluding outliers.

Velocity profiles were simultaneously measured using two Lowered Acoustic Doppler Current Profiler (LADCPs) Teledyne 300 kHz narrowband units mounted on the CTD frame. One unit faced upwards and the other downwards to maximize the total range of velocity observations. Each instrument was configured with 20 bins, each 8 m in length, which allowed for a measurement range of ~160 m (Thurnherr, 2010). The raw LADCP data were processed using the LDEO Software version IX by applying the least-squared method, using the navigation and the vessel-mounted (VM) ADCP data as constraints (Visbeck, 2002).

#### 3.1.2. Vessel-mounted (VM) ADCP data

The R/V *Garcia del Cid* was equipped with a vessel-mounted (VM) 75 kHz ADCP (Ocean Surveyor, RD Instruments) that recorded current velocities along the hydrographic sections. The VM-ADCP was configured to record current velocities at 2-min averages, while sampling depths were set to 8-m vertical bins. The VM-ADCP data were processed using the CASCADE V7.2 software (Le Bot et al., 2011). Absolute current velocities resulted from removing the vessel speed, derived

from a differential global positioning system. The measurement range of the instrument was from 20 m to 720 m depth. Given the micro-tidal regime of the Mediterranean Sea (tidal range ~ 0.5 m), tides are considered of very low magnitude in the GoL (Davis and Hayes, 1984; Dipper, 2022). Nevertheless, a barotropic tide correction was applied to the VM-ADCP data using the OTIS-TPX8 Tide model (<a href="https://www.tpxo.net/global">https://www.tpxo.net/global</a>) within the cascade V7.2 software, which provided tide-corrected current velocities. VM-ADCP data were then screened to align with the timeframe of the different hydrographic sections. However, the VM-ADCP's range could not fully cover the water column due to the interaction of secondary acoustical lobes with the seabed. To address this limitation, we integrated VM-ADCP data with LADCP measurements recorded at each station. This integration involved aligning time stamps, matching coordinate systems, and merging and interpolating datasets.

Finally, ADCP velocities, decomposed into E-W and N-S components, were rotated 15° counterclockwise to align with the local canyon axis orientation. This rotation provided the across- and along-canyon velocity components for interpretation. For the across-canyon component, eastward velocities have been defined as positive and westward velocities as negative. For the along-canyon component, up-canyon velocities are positive, while down-canyon velocities are negative.

#### 3.1.3. Glider observations

. 

The hydrodynamics of dense shelf waters at the continental shelf adjacent to the Cap de Creus Canyon were monitored by a SeaExplorer underwater glider (ALSEAMAR-ALCEN). The glider carried out one along-shelf (i.e., north-south) section and navigated 10 km for 25 hours, starting on March 5, 2022 (Fig. 1b). It conducted a total of 28 yos (down/up casts). It followed a sawtooth-shaped trajectory through the water column, descending typically to 2 m above the bottom (between 83 and 92 m depth) and ascending to 0-1 m of distance from the surface. The glider was equipped with a pumped SeaBird GPCTD, coupled with a dissolved oxygen sensor (SBE43F), that acquired temperature, conductivity, and pressure data at a sampling rate of 4s. Additionally, the glider had a SeaBird Triplet (WetLabs FLBBCD sensor), which measured proxies of phytoplankton abundance (by measuring the fluorescence of chlorophyll-a at 470/695 nm), and total particle concentration (by measuring optical backscattering at 700 nm). Finally, the glider integrated a downward-looking AD2CP (Acoustic Doppler Dual Current Profiler) that measured relative water column velocities and the glider speed. The AD2CP was configured with 15 vertically stacked cells of 2 m resolution, and a sampling frequency of 5 s. Raw velocity measurements were processed using the shear method to derive absolute current velocities (Fischer and Visbeck, 1993; Thurnherr et al., 2015; Homrani et al., 2025). We used bottom tracking and GPS coordinates as constraints to reference each velocity profile.

The hydrographic profiles obtained from the glider were similarly interpolated using the isopycnic gridding method as applied to the CTD data (Schlitzer, 20222023).

#### 3.2. Ancillary data

#### 3.2.1. Environmental forcings and shelf observational data

Heat flux data were used to evaluate the interaction between the atmosphere and the ocean surface. Data were retrieved from the European Centre for Middle-range Forecast (ECMWF) ERA5 reanalysis by Copernicus Climate Change Service. This global reanalysis product provides hourly estimates of a large number of atmospheric variables since 1940, with a horizontal resolution of 0.25 ° (Hersbach et al., 2023). For this study, the sea-atmosphere interactions were assessed from 42.6 °N to 43.4 °N and from 3 °E to 4.5 °E, approximately covering the entire GoL's continental shelf, from October 2021 to July 2022.

Significant wave height (Hs) data were retrieved from the Banyuls buoy (06601) located at 42.49 °N and 3.17 °E (Fig. 1b), through the French CANDHIS database (<a href="https://candhis.cerema.fr">https://candhis.cerema.fr</a>). These measurements were recorded every 30 min using a directional wave buoy (Datawell DWR MkIII 70). Wind speed and direction data were obtained from the POEM buoy (<a href="https://www.seanoe.org/data/00777/88936/">https://www.seanoe.org/data/00777/88936/</a>; Bourrin et al., 2022), which records hourly observations using a surface meteorological sensor and is also equipped with a multiparametric CTD probe measuring near-surface temperature and salinity.

In addition, the SOLA station, located in the Bay of Banyuls-sur-Mer (Fig. 1) and managed by the SOMLIT network (<a href="https://www.seanoe.org/data/00886/99794/">https://www.seanoe.org/data/00886/99794/</a>; Conan et al., 2024) provided weekly near-bottom (~27 km) time series of temperature, salinity, and pressure. This data allowed to monitor the presence of dense shelf waters over the continental shelf during the winter of 2021-2022. Raw data were processed to remove gaps and outliers prior to analysis.

Water discharge of rivers opening to the GoL was measured by gauging stations located near rivers mouths and provided by Hydro Portail v3.1.4.3 (<a href="https://hydro.eaufrance.fr">https://hydro.eaufrance.fr</a>). For this study, we have considered the river discharge from the Rhône River and the total discharge from coastal rivers as the sum of their individual contribution.

## 3.2.2. Instrumented mooring lines

Current velocity and direction, temperature, and SPM concentration were monitored in two submarine canyons, the Lacaze-Duthiers Canyon (LDC) and the Cap de Creus Canyon (CCC), by means of two instrumented mooring lines (Fig. 1b). The mooring line at Lacaze-Duthiers Canyon, located at about 1000 m depth, has been maintained in the canyon since 1993 as part of the MOOSE program. It is equipped with two current meters (Nortek Aquadopp 2 MHz) with temperature, conductivity, and turbidity sensors, placed at 500 m and 1000 m depth (referred to as LDC-500 and LDC-1000, respectively). The sampling interval for the current meters was set to 60 min. The fixed mooring line at the Cap de Creus Canyon has been maintained in the canyon axis by the University of Barcelona since December 2010. This mooring line, referred to as CCC-1000, is equipped with a current meter (Nortek Aquadopp 2 MHz) with temperature, conductivity, and turbidity sensors placed at 18 m above the bottom (mab). The current meter sampling interval was set to 15 min. For this study, the recording period was considered from December 1, 2021 to April 1, 2022, which encompassed the winter of 2021-2022.

#### 3.3. Determination of suspended particulate matter (SPM) concentrations from turbidity measurements

To calibrate turbidity measurements obtained in the Cap de Creus Canyon during the FARDWO-CCC1 Cruise, water samples were collected at selected depths with Niskin bottles. For each sample, between 2 and 3 L of water were vacuum filtered into 47 mm 0.4  $\mu$ m pre-weighted Nucleopore filters. The filters were then rinsed with MiliQ water to remove salt and stored at 4 °C. Then, these filters were dried by desiccation and weighted. The weighing difference of the filters divided by the volume filtered of seawater yielded to the SPM concentration, in mg·L-1. Finally, the measured SPM concentrations were plotted against in situ turbidity measurements, both from the transmissometer and the optical sensor (Figs. 2a, b). The beam attenuation coefficient (BAC) from the transmissometer showed a stronger correlation with SPM (R<sup>2</sup> = 0.86) compared to FTU from the SeaPoint turbidity sensor (R<sup>2</sup> = 0.81). Therefore, SPM concentrations were predicted using the equation:

SPM = 
$$1.84 \cdot BAC + 0.05$$
 ( $R^2 = 0.85$ ;  $n = 25$ ) (1)

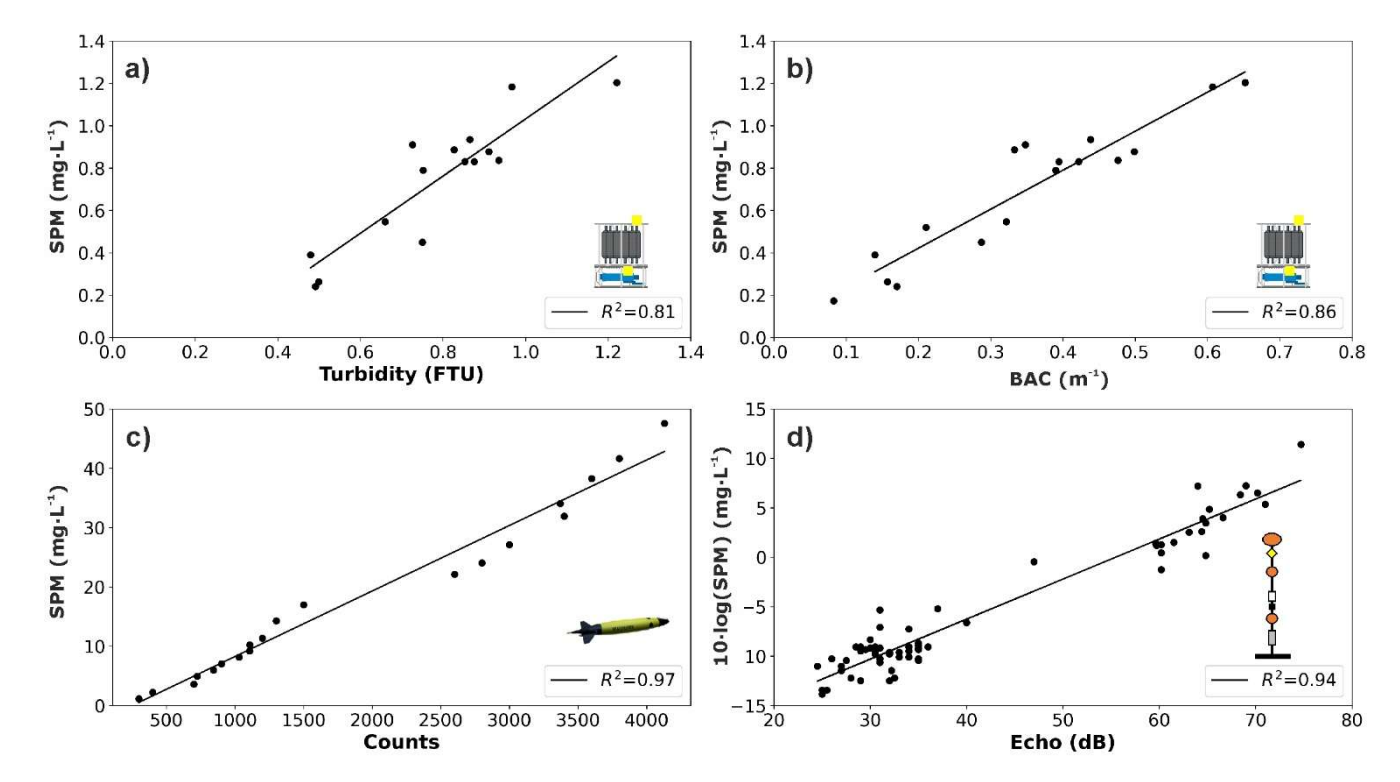


**Figure 2.** Relationship between the weighed SPM mass concentration (mg·L<sup>-1</sup>) and: (a) turbidity records (FTU) from the SeaPoint sensor and (b) BAC (m<sup>-1</sup>) from the WetLabs transmissometer attached to the CTD-rosette system; (c) optical backscatter sensor data (counts) from the WetLabs FLBBCD sensor mounted on the SeaExplorer glider; (d) echo intensity (dB) retrieved from the current meters installed in LDC and CCC instrumented moorings. For each relationship, the regression coefficient (R<sup>2</sup>) is given.

**\$02** 

Backscatter data (in counts) from a self-contained FLBBCD optical sensor, identical to the one installed on the SeaExplorer glider, were also correlated to SPM concentration using a laboratory calibration. Firstly, the optical sensor was submerged into a 10-L plastic tank filled with freshwater. Then, sediment was added while stirring the water to distribute the sediment particles evenly. The amount of sediment was gradually increased until the instrument reached a saturation level of approximately 4,000 counts, corresponding to a sediment mass of 447.5 mg. The optical sensor, connected to a computer, displayed and stored the turbidity measurements during the calibration process. Then, water samples were taken at each interval and filtered, obtaining SPM concentration (in mg·L<sup>-1</sup>). Pairs of counts/SPM data points yielded the following regression line (Fig. 2c):

SPM = 
$$0.01 \cdot \text{counts}$$
 (R<sup>2</sup> =  $0.97$ ; n = 20) (2)

Finally, echo intensity (EI) records from the current meters equipped in LDC and CCC lines were also correlated with SPM concentration, using a linear equation relating the logarithm of SPM to EI (Gartner, 2004). Unlike optical devices, acoustic sensors measure relative particle concentrations based on changes on the backscattered acoustic signal (Fugate and Friedrichs, 2002). Acoustic backscatter, expressed in counts, is proportional to the decibel sound pressure level (Lohrmann, 2001), and depends on the particle size and on the operating frequency of the acoustic sensor (Wilson and Hay, 2015). The equation derived from the regression between backscatter data and direct sampling concentration in the GoL was (Fig. 2d):

$$10 \cdot \log (SPM) = 0.405 \cdot EI - 22.46 (R^2 = 0.94; n = 66)_{(3)}$$

#### 3.4. Estimation of dense water and SPM transports from observations

The total transports of dense shelf water and associated SPM were estimated using hydrographic and current measurements collected during the FARDWO-CCC1 cruise and the glider survey conducted in early March 2022 in the Cap de Creus Canyon and its adjacent shelf, respectively.

First, to isolate dense shelf waters, we selected water masses with a potential temperature below  $12.9\,^{\circ}$ C and potential density below  $29.\underline{105}\,\mathrm{kg\cdot m^{-3}}$ . At the canyon, these properties already corresponded to the signature of the Western Intermediate Water (WIW). Then, dense water transport (expressed in  $\mathrm{Sv} = 1\cdot10^6\,\mathrm{m^3\cdot s^{-1}}$ ) was calculated by integrating the zonal component of current speed (which aligns with the down-canyon direction) over the area-depths occupied by dense waters. For the T1 and T2 transects, current speed was measured using the LADCP attached to the CTD-rosette system, and transport was calculated in vertical cells of 8 m (the LADCP bin size) and then integrated over the whole transect. For the glider section over the continental shelf, dense water transport was computed using the same approach, although current velocity data were obtained from the glider-mounted AD2CP.

After estimating dense water transport, we computed the associated SPM transport (in metric tons) by multiplying the calculated water transport by the SPM concentration within the dense water layer. SPM concentrations were derived from the SeaPoint sensor integrated into the CTD probe for the canyon transects, and from the WetLabs FLBBCD sensor onboard the glider for the shelf section. Finally, all SPM profiles were resampled to match the vertical resolution of current velocity measurements prior to integration.

# 3.5. Reanalysis data

**\$19** 

₿42

**\$45** 

To complement the observational dataset, we used the Mediterranean Sea Physics Reanalysis (hereafter MedSea) from the Copernicus Marine Service to evaluate the spatiotemporal evolution of hydrographic properties and transport patterns of dense shelf waters in the Cap de Creus Canyon. This reanalysis product has a horizontal resolution of 1/24° (~4-5 km) and provides daily estimates of ocean variables, including temperature, salinity, and currents at multiple depths (Escudier et al., 2020, 2021).

First, we used the MedSea data to assess the temporal evolution of hydrographic conditions during winter 2021-2022. Daily time series of temperature and salinity were extracted from two grid points at key locations along the pathway of dense waters: one located at the shelf break (RA-SB: 42.48 °N and 3.29 °E, depth= 250 m), and another within the Cap de Creus Canyon (RA-C: 42.34 °N and 3.37 °E, depth= 350 m) (Fig. 1b).

Then, we calculated the transport of dense shelf waters through the canyon using MedSea data by applying the same approach as for the observational dataset. First, we identified dense shelf waters using the same hydrographic thresholds (T < 12.9 °C and  $\sigma$  < 29.05–1 kg·m<sup>-3</sup>). Then, we estimated the dense water transport (in Sv) by integrating the zonal velocity component (aligned with the downcanyon direction) across two virtual transects close to the T1 and T2 sections sampled during the FARDWO-CCC1 cruise (Fig. 1b). This analysis was performed for the winter of 2021-2022 to capture the temporal variability of the transport, and allowed us to extend the analysis beyond the limited period covered by the field data. Finally, to determine the temporal context and interannual variability of dense shelf water transport, we analyzed a 26-year (1997-2022) time series of MedSea reanalysis data across a central transect in the Cap de Creus Canyon (see location in Figure 1). Dense waters were identified by temperature < 12.9 °C and zonal velocity > 0.1 m·s<sup>-1</sup> (down-canyon velocities). We distinguished IDSWC events by a density threshold > 29.1 kg·m<sup>-3</sup>, whereas MDSWC events were characterized by densities below this threshold. This long-term analysis allowed us to place the 2021–2022 MDSWC event in the context of other cascading episodes previously reported in the Gulf of Lion and to evaluate its relative intensity.

**\$54** 

\$55

356

\$57

\$58

359

360

\$61

362

363

364

365

366

\$67

\$68

369

\$70

**\$71** 

\$72

**\$73** 

\$74

**375** 

**\$76** 

**\$77** 

**\$78** 

**\$**79

\$80

381

382

383

**384** 

**\$85** 

386

**\$87** 

\$88

\$89

\$90

\$91

₿92

# 4.1. Meteorological and oceanographic conditions during winter 2021-2022

The meteorological, oceanographic, and hydrological conditions during winter 2021-2022 are summarized in Figure 3. In order to understand the thermohaline characteristics observed in the Cap de Creus Canyon during the FARDWO-CCC1 cruise in a broader temporal and spatial context, near-bottom temperature, salinity, and potential density at the shelf, shelf break, and canyon for the entire winter of 2021-2022 are also shown in Fig. 3.

The time series of net heat fluxes over the GoL's shelf showed negative values from October 2021 to early April 2022, indicating a heat loss from the ocean to the atmosphere (Fig. 3a). The strongest net heat losses during that winter occurred between in-November 2021 and late February January 2022, reaching values of about -400 W·m<sup>-2</sup> (Fig. 3a). As usual in the study area during winter, the most frequent and generally strongest winds were northern and northwesterly winds (Tramontane and Mistral), alternated with shorter periods of easterly and southeasterly winds (Fig. 3b). The duration of these-northerly and northwesterly winds events varied throughout the season, from short

blowing in short bursts of 1-3 days to 3 days during in October and December to, and in longer periods of 5-7 to 7 consecutive days during in November and February (Fig. 3b), with occasional peaks. The highest wind speeds during this period exceedinged 20-25 m·s·¹ and were associated with the strongest strong heat losses (Figs. 3b, c). A period of sustained northerly winds during February, with wind speeds up to 20 m·s·¹, preceded and continued through the FARDWO-CCC1 cruise (1-7 March) (Figs. 3b, c). During this period, Ssignificant wave height (Hs) ranged between 0.5 and 2.0 m·during winter, with no major marine storms recorded before or during the cruise (Fig. 3c). In parallel, tThe mean water discharge of the Rhône River discharge generally displayed average -values of about 1850 m³·s·¹ (Fig. 3d; Pont et al., 2002; Provansal et al., 2014), while -Ccoastal river discharges remained relatively low throughout the entire winter, typically below 200 m³·s·¹ (Fig. 3d; Pont et al., 2002; see average daily water discharge values in Bourrin et al., 2006), typically below 200 m³·s·¹ (Fig. 3d; Pont et al., 2002; see average daily water discharge values in Bourrin et al., 2006), typically below 200 m³·s·¹ . This period of strong heat losses, combined with persistent northerly and northwesterly winds, represent the typical winter conditions that favor the formation of dense shelf waters in the Gulf of Lion (Durrieu de Madron et al., 2005). This period of strong heat losses, combined with persistent northerly and northwesterly winds, represent the typical winter conditions that favor the formation of dense shelf waters in the Gulf of Lion.

After the cruise, a series of sustained eastern winds occurred during March and April 2022 (Fig. 3b). From mid-March onwards, easterly winds were more frequent than at any other time of winter 2021-2022 and were particularly intense on March 11-13, with speeds of ~19 m·s<sup>-1</sup> (Fig. 3b). In particular, the eastern storm on March 13 was accompanied with Hs > 3 m, which lasted for over 20 hours (Fig. 3c). The sustained easterly winds during March 11-13 pulled Mediterranean humid air towards southern France, causing intense rainfall from the Eastern Pyrenees to the Massif Central. In contrast, precipitations in the rest of France, including the watershed of the Rhône River, were weak (https://www.eaufrance.fr/publications/bsh/2022-04). As a consequence, coastal river discharges increased up to 2265 m³·s<sup>-1</sup>, while the Rhône River discharge was comparatively lower (884 m³·s<sup>-1</sup>) (Fig. 3d).

The hydrographic conditions during winter 2021-2022 revealed the presence of dense shelf waters at the shelf, shelf break and canyon from late January to early March, prior to the FARDWO-CCC1 cruise (Figs. 3e-g). During this period, only one marine storm, defined as sustained Hs > 2 m for more than 6 hours (Mendoza and Jimenez, 2009), was recorded on March 13, 2022. This storm was associated with an easterly/south-easterly wind event with maximum speeds of ~19 m·s<sup>-1</sup>, and generated Hs > 3 m for over 20 hours (Fig. 3c).

The mean water discharge of the Rhône River generally displayed average values of about 1850 m³-s¹- (Fig. 3d; Pont et al., 2002; Provansal et al., 2014). However, the discharge exceeded 2000 m³-s¹- during early October, early November, and mid-December 2021 (Fig. 3d). A peak discharge of over 5000 m³-s¹- occurred in late December, associated with a brief easterly/south easterly wind event (Fig. 3c). Coastal river discharges remained relatively low throughout winter (see average daily water discharge values in Bourrin et al., 2006), typically below 200 m³-s¹-, except for a few short episodes when river discharge exceeded 400 m³-s¹- (Fig. 3d). The highest coastal river discharge occurred on March 13, 2022, after a period of sustained easterly/southeasterly winds (Fig. 3c). During this event, the coastal river discharges reached 2265 m³-s¹-, surpassing the water discharge of the Rhône River, which was comparatively lower (884 m³-s¹-) (Fig. 3d).

393

394

\$95

396

**\$**97

398

399

400

401

402

403

404

405

406

407

408

409

410

411

412 413

414

415

416

417

418

419

420

421

422

The nNear-bottom temperature time series at the continental shelf, measured by the POEM buoy, showed a gradual decreased gradually decline from 20 °C in October 2021 to to 13 °C during wintertime in March 2022 (Fig. 3e), while . Ssalinity fluctuated between 37.8 to 38.1 during this period, occasionally dropping below 37.8 in parallel with temperature decreases (Fig. 3f). At the shelf break (250 m depth) and in the Cap de Creus Canyon (350 m depth), reanalysis data showed generally stable thermohaline properties, with short-lived pulses of colder (12.9 °C) waters from late January to early March (Figs. 3e, f). Potential density Near-bottom temperature and salinity time series at the shelf break (250 m depth) and at the Cap de Creus Canyon (350 m depth), as previously noted, were derived from reanalysis data. At the shelf break, temperature remained constant around 14.5 °C, except for an increase to 15.5 °C throughout November and a subsequent decrease below 13 °C from January to late March 2022 (Fig. 3e). Salinity at the shelf break also remained constant (~38.55) throughout winter (Fig. 3f). At the Cap de Creus Canyon, temperature and salinity remained stable around 14.5 °C and 38.8, respectively, during winter. From late January to late March 2022, both variables occasionally dropped in short lived pulses to 12.9 °C and 38.1, respectively, before returning to baseline values (Figs. 3e, f). The potential density anomaly at the shelf and shelf break followed the seasonal temperature variations, and it only increased during February-March 2022 when it peaked at ~28.9 kg·m<sup>-</sup> <sup>3</sup> (Fig. 3g), while density at the canyon remained relatively constant (28.8-28.95 kg·m<sup>-3</sup>) throughout winter. In contrast, density at the Cap de Creus Canyon remained relatively stable, slightly varying between 28.75 and 28.95 kg·m<sup>-3</sup> throughout the study period (Fig. 3g)...

From March to May 2022, the wind pattern alternated between northerly/north westerly winds and short intervals (2-4 days) of easterly/southeasterly winds (Fig. 3b). Similar to winter, the strongest heat losses occurred in April 2022, and coincided with a relatively long period (5 days) of northerly/north-westerly winds with speeds above 20 m·s<sup>-1</sup> (Figs. 3a, b).

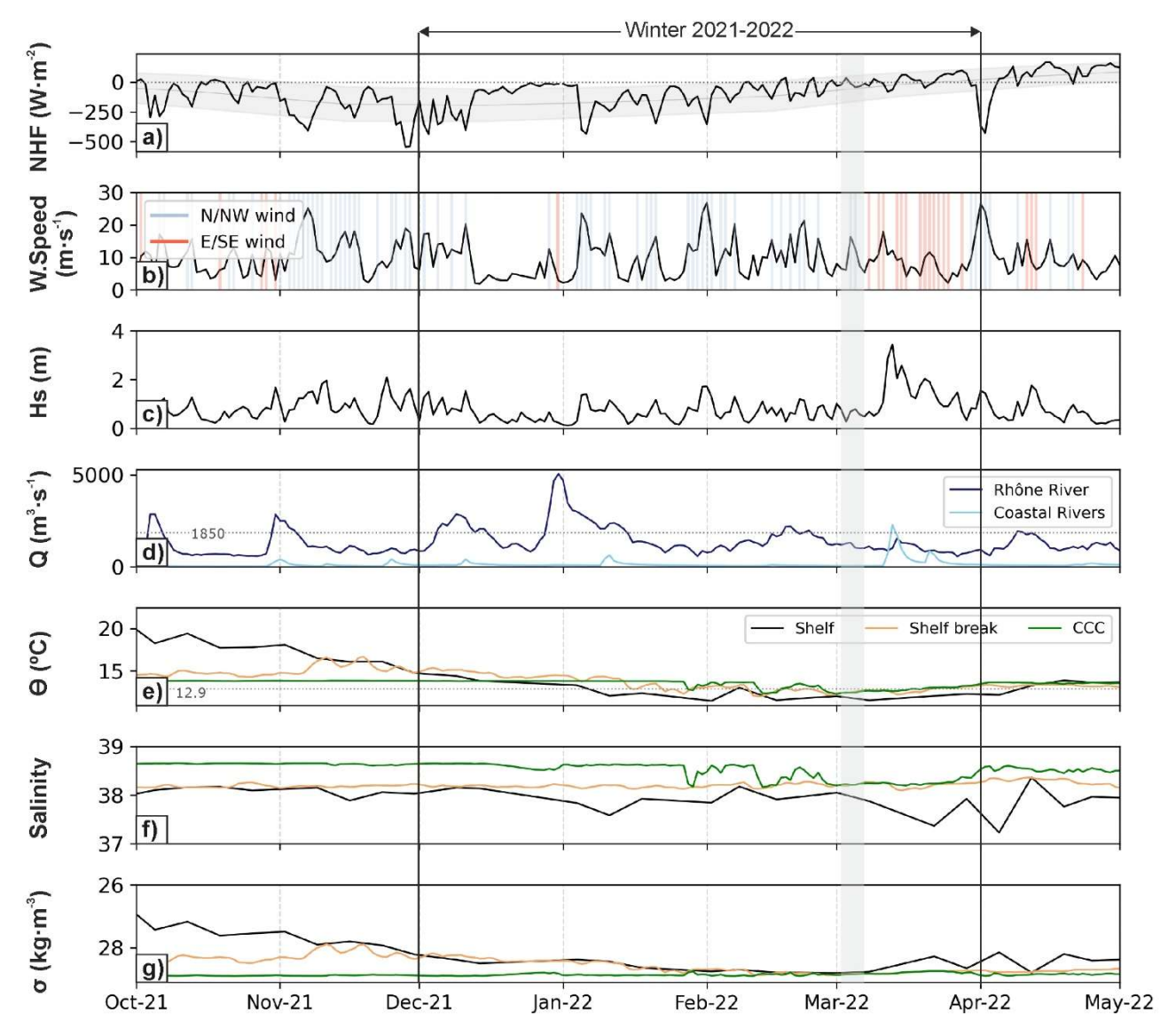


**Figure 3.** Time series of (a) net heat fluxes (NHF, W·m<sup>-2</sup>) averaged over the GoL's shelf; (b) wind speed (m·s<sup>-1</sup>) measured at the POEM buoy. Blue and red shaded bars indicate N/NW and S/SE winds, respectively; (c) significant wave height (Hs, m) measured at the Banyuls buoy; (d) river discharge (Q, m³·s<sup>-1</sup>) of the Rhône River (dark blue) and coastal river discharges discharging into the GoL (light blue); (e) weekly mean bottom temperature ( $\theta$ , °C), (f) salinity, and (g) potential density ( $\sigma$ , kg·m<sup>-3</sup>) calculated from *TS* data at the continental shelf (black), the shelf break (orange), and the Cap de Creus Canyon (green). Data at the continental shelf were measured at the POEM buoy. Data at the shelf break and within the Cap de Creus Canyon were extracted from two grid points from the MedSea. All data are displayed for the period between October 2021 and May 2022. The grey shaded vertical bar highlights the FARDWO-CCC1 Cruise, which took place on March 1-7<sup>th</sup>, 2022. The studied winter period is also indicated in the figure and corresponds to the time of most negative NHF values, indicating the strongest ocean heat loss to the atmosphere and favorable conditions for DSWC events.

#### 4.2. Time series at Lacaze-Duthiers and Cap de Creus canyons during winter 2021-2022

 Figure 4 shows the time series of temperature, current speed and direction, and SPM concentration recorded at the mooring stations in Lacaze-Duthiers Canyon (at 500 and 1000 m depth) and the Cap de Creus Canyon (at 1000 m depth) during winter 2021-2022. At 500 m depth in Lacaze-Duthiers Canyn (LDC-500), temperature remained relatively constant between 13.5 and 14 °C, while at 1000 m in both Lacaze-Duthiers and Cap de Creus canyons, it fluctuated between 13.1 and 13.4 °C (Fig. 4a). Current speeds ranged from 0.01 to 0.1 m·s<sup>-1</sup> at 500 in Lacaze-Duthiers Canyon and at 1000 m in the Cap de Creus Canyon (Figs. 4b, d), and from 0.1 and 0.2 m·s<sup>-1</sup> at 1000 m in Lacaze-Duthiers Canyon (Fig. 4c). At this depth,

current speed increased several times to 0.12 m·s<sup>-1</sup> between January and mid-March 2022, and peaked at 0.2 m·s<sup>-1</sup> in late March (Fig. 4c). A similar, but less intense peak was observed in the Cap de Creus Canyon at 1000 m during the same period (Fig. 4c), coinciding with small temperature drops (Fig. 4a). Current direction at 500 m in Lacaze-Duthiers Canyon was isotropic (Fig. 4b), while at 1000 m in both Lacaze-Duthiers and Cap de Creus canyons, it became anisotropic and preferentially aligned with the orientation of the respective canyon axes (Figs. 4c, d). The time series of SPM concentrations ranged between 0.2 and 0.5 mg·L<sup>-1</sup> at all monitored depths at all mooring sites during winter 2021-2022 showed values ranging between 0.2 and 0.5 mg·L<sup>-1</sup> at all monitored depths (Fig. 4e). The highest SPM concentrations were recorded at 1000 m depth in the Cap de Creus Canyon from mid-February to late March 2022, reaching values of ~ 1 mg·L<sup>-1</sup> (Fig. 4e). In general, temperature, current speed and direction, and SPM concentrations showed small variability prior to the FARDWO-CCC1 cruise, and the arrival of dense shelf waters was not clearly observed at the monitored depths (Fig. 4).

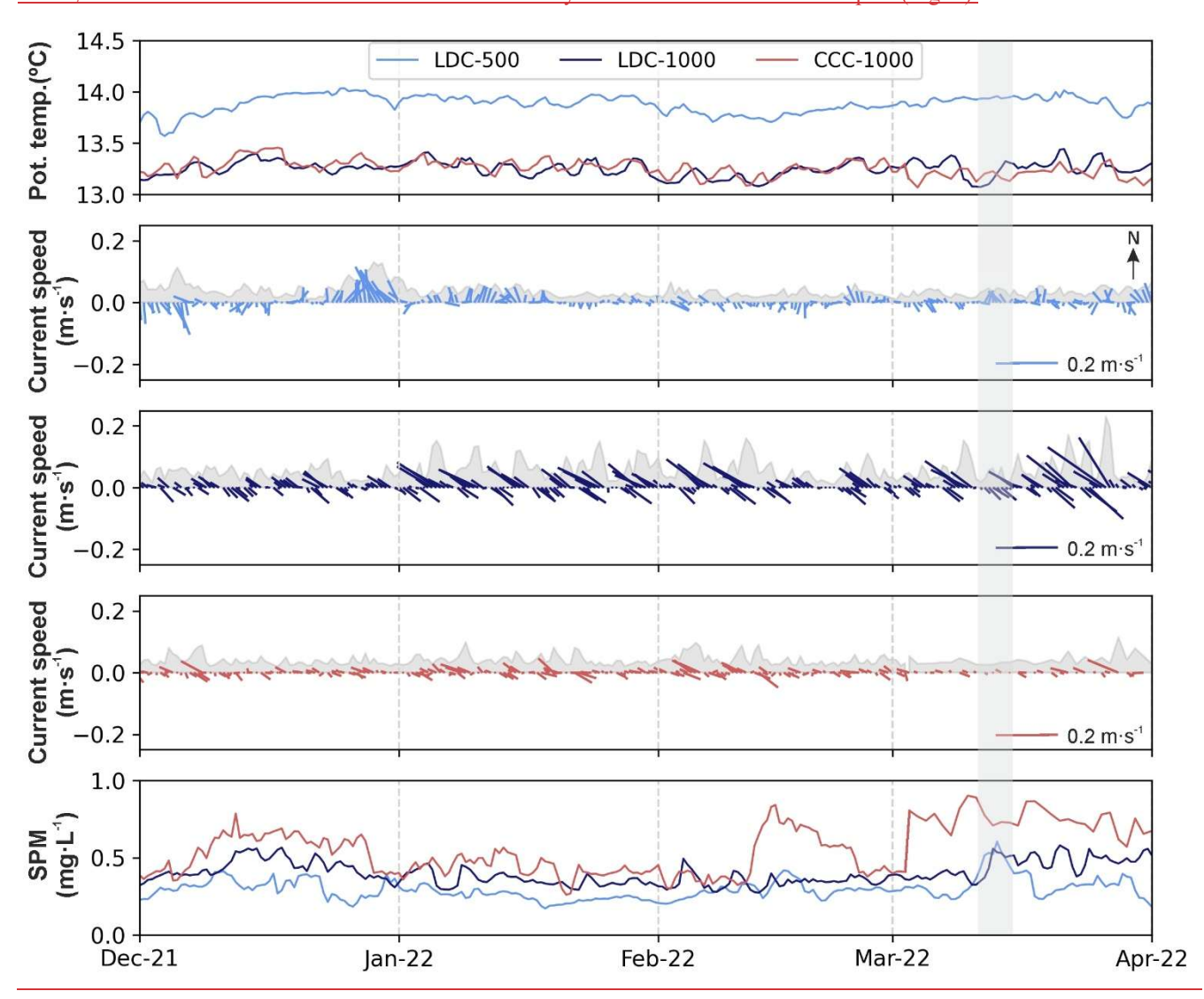


**Figure 4.** Time series of (a) potential temperature (°C), (b-d) stick plots of currents and current speed as a shaded grey area (m·s<sup>-1</sup>), and (e) suspended particulate matter concentration (SPM, mg·L<sup>-1</sup>) measured at the mooring stations in Lacaze-Duthiers Canyon (LDC-500 in light blue, and LDC-1000 in dark blue) Cap de Creus Canyon (CCC-1000 in red) during winter 2021-2022. In panels (b-d), arrows indicate the along-canyon component for each mooring site. The grey shaded vertical bar highlights the FARDWO-CCC1 Cruise, which took place on March 1-7, 2022.

#### 4.3. Water column properties at the Cap de Creus Canyon and adjacent shelf in March 2022

#### 4.3.1. Hydrographic and biogeochemical properties

The continental shelf adjacent to the Cap de Creus Canyon was monitored on March 5 with, using a SeaExplorer glider, which profiled which monitored the water column from the surface down to 92 m depth. In the northern part of the shelf transect, a water mass characterized with temperatures of by temperatures of 12.9 °C and salinities of 38.2 occupied most of the water column above the 28.95 kg·m<sup>-3</sup> isopycnal (Figs. 5a-c). This water mass exhibited showed SPM concentrations of 1.5-3.0 mg·L<sup>-1</sup> and dissolved oxygen values values of ~232 µmol·kg<sup>-1</sup> (Figs. 6a, c). Near the bottom, a relatively cooler, fresher, and more turbid, and oxygen-richer water mass with higher dissolved oxygen concentrations was observed in the northern part of the section (Figs. 5a-c and 6a-c). This water mass flowed along the shelf below the 28.95 kg·m<sup>-3</sup> isopycnal, gradually becoming slightly warmer, saltier, less turbid, and less oxygenated towards the southern part of the shelf transect (Figs. 5a-c and 6a-c). Fluorescence values also generally increased towards the southern-southward along the part of the shelf transect (Fig. 6b). Altogether, tThese hydrographic and biogeochemical properties clearly indicate the presence of dense shelf waters on the continental shelf in the shape of a wedge that thickened towards the Cap de Creus Peninsula (i.e., south) near the bottom (Figs. 5a-c and 6a-c). These results conditions reflect represent the oceanographic conditions on of the continental shelf shortly before the start-onset of the FARDWO-CCC1 cruise.

During the FARDWO-CCC1 cruise, two ship-based CTD transects were conducted across the Cap de Creus Canyon. The T1 transect, \_was-carried out across the upper \_canyon, \_section of the canyon, \_extended\_ from the surface down to 625 m depth. The upper \_100 m\_water\_column (< 100 m\_depth) was\_were\_ characterized by temperatures of 13-13.2 °C, salinities of ~38.25 (Figs. 5d, e), dissolved oxygen concentrations of ~200 μmol·kg-¹, and relatively low SPM concentrations (0.3 mg·L-¹) (Figs. 6d, f). Beneath this layer, a colder (12.2-12.7 °C), fresher (S = 38.1-38.2) water mass was observed detaching from the southern flank into the canyon interior at occupied depths of 100-400 m\_depth, along the southern flank of the canyon (Fig. 5d, f), with densities ~29 kg·m-³, \_This water mass showed relatively high dissolved oxygen values (>~200 μmol·kg-¹), and increased SPM concentrations (1-1.2 mg·L-¹) (Figs. 6d-f). It extended ~3 km into the canyon interior. Fluorescence values were generally high (0.5-1.1 μg·L-¹) in the upper 400 m of the water column, while they decreased towards the bottom (Fig. 6e). Below, a relatively cooler, saltier, less oxygenated, and slightly denser (~29.55 kg·m-³) water mass was apparent around 350-400 m depth (Figs. 5d-f). Deeper into the canyon (At depths > 400 m\_depth), a much warmer (T > 13 °C) and saltier (S ~ 38.4) water mass with lower SPM concentrations (~0.4 mg·L-¹) and fluorescence values was observed (Figs. 5d-f and 6d-f).

Further downcanyon, the T2 transect crossed the middle section of the <u>canyon Cap de Creus Canyon</u>, <u>covering and covered</u> the <u>entire</u> water column down to 850 m depth (Figs. 5g-i and 6g-i). The upper 250 m <u>showed a were</u> remarkably homogeneous, <u>with</u> <u>water mass throughout the canyon. It was characterized by</u> temperatures of 13.2-13.4 °C, salinities of ~38.2, <u>relatively high</u> dissolved oxygen values (~197 μmol·kg<sup>-1</sup>), and low SPM concentrations (0.3 mg·L<sup>-1</sup>) (Figs. 5g-i and 6g-i). Below this layer, <u>between and down 250 and to 380 m depth</u>, a much colder (12.2-12.3 °C), fresher (38.1), highly oxygenated (200-203 μmol·kg<sup>-1</sup>) and moderately turbid (0.8-1.0 mg·L<sup>-1</sup>) water mass was observed <u>detaching from the southern canyon flank</u> (Figs. 5g-i and 6g-i). <u>Its density ranged 28.9-29.0 kg·m<sup>-3</sup> (Fig. 5j), and This water mass only occupied the southern flank of the canyon and extended approximately 2.5 km into the interior of the canyon (Figs. 5g i and 6g i). <u>Ffluorescence values throughout this layer</u> ranged from 0.18 to 0.60 μg·L<sup>-1</sup> throughout the canyon from the surface to ~380 m depth above the 29.0 kg·m<sup>-3</sup> isopycnal (Fig. 6h). Finally, between from 400 m and to 850 m depth, the water column showed a water mass was characterized by with temperatures of ~13.1 °C, salinities of 38.4, and relatively lower oxygen concentrations, fluorescence values, and SPM concentration (Figs. 6g-i).</u>

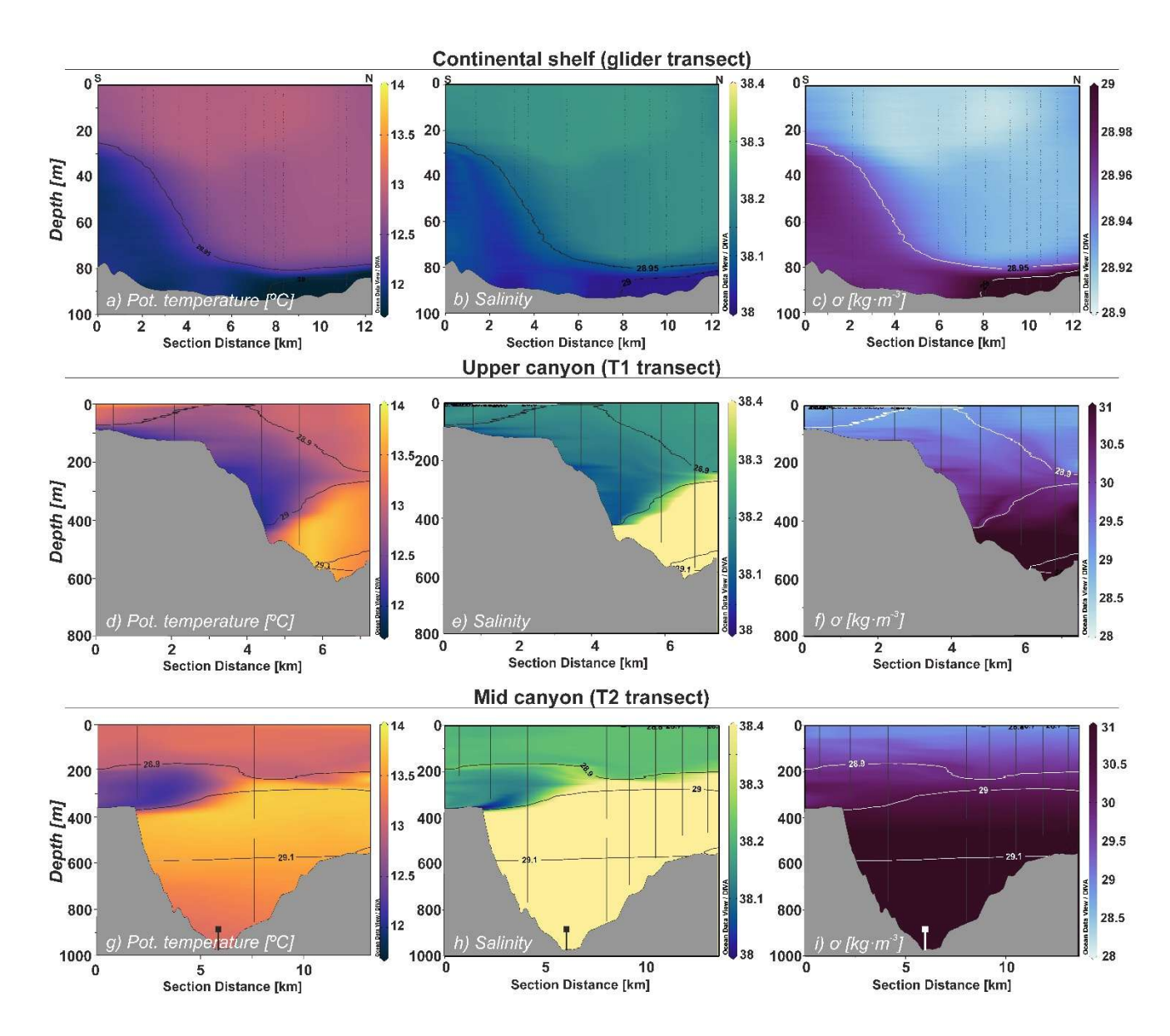


**Figure 5.** Contour plots of potential temperature ( ${}^{\circ}$ C), salinity, and potential density ( $\sigma$ , kg·m<sup>-3</sup>) at (a-c) the continental shelf (glider transect) and the Cap de Creus Canyon during (d-f) T1 transect and (g-i) T2 transect (FARDWO-CCC1 cruise). Note that for panels (a-c), the section distance goes from south to north, whereas for panels (d-i), the section distance represents a southwest-northeast direction. Note the change in the density scale in panel (c).

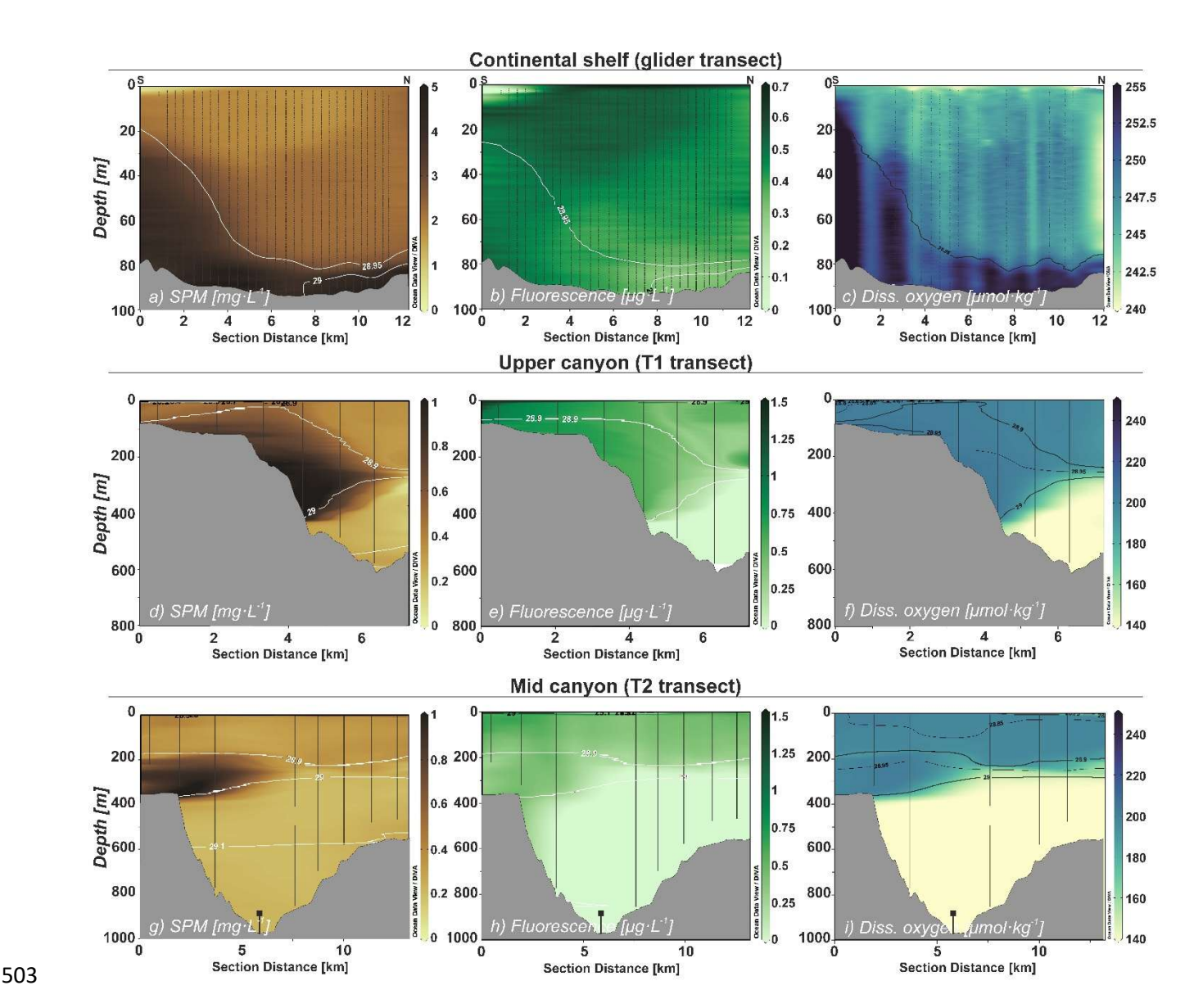


**Figure 6.** Contour plots of SPM concentration (mg·L<sup>-1</sup>), fluorescence (μg·L<sup>-1</sup>), and dissolved oxygen concentration (μmol·kg<sup>-1</sup>) at (a-c) the continental shelf (glider transect) and at the Cap de Creus Canyon during (d-f) T1 transect and (g-i) T2 transect (FARDWO-CCC1 cruise). Note that for panels (a-c), the section distance goes from south to north, whereas for panels (d-i) the section distance represents a southwest-northeast direction. Note the change in the dissolved oxygen scale in panel (c).

#### 4.3.2. Currents

\$12

At the continental shelf, current velocity measurements indicated a fairly homogeneous current field (Figs. 7a-c). Cross-shelf currents exhibited low velocities (< 0.1 m·s<sup>-1</sup>), predominantly eastward (Fig. 7a), while along-shelf currents were slightly higher (0.1-0.15 m·s<sup>-1</sup>) and predominantly southward (Fig. 7b). The spatial distribution of currents averaged within the dense water plume (defined between the 28.9 and 29.10 kg·m<sup>-3</sup> isopycnals) shows that dense shelf waters flowed south/south-eastward along the continental shelf adjacent to the Cap de Creus Canyon, with speeds generally around 0.15 m·s<sup>-1</sup> (Fig. 7c). However, in the southern part of the section, currents were stronger, exceeding 0.2 m·s<sup>-1</sup> (Fig. 7c).

In the Cap de Creus Canyon, at the upper section (T1 transect), current velocity measurements revealed the highest speeds from the surface to 400 m depth at the southern canyon flank (Figs. 7d, e). The zonal current velocity (E-W) reached up to 0.3 m·s<sup>-1</sup> eastward (Fig. 7d), while the meridional current velocity (N-S) was primarily southward, with velocities between 0.1 and 0.2 m·s<sup>-1</sup> (Fig. 7e). These currents appeared relatively confined within the canyon axis, with a pronounced down-canyon component (Fig. 7f). At the mid-canyon section (T2 transect), the highest current velocities were observed between 200 and 400 m depth (Figs. 7g, h). The zonal current velocities were more pronounced, and reached values of ~0.15

34

 $m \cdot s^{-1}$  eastward (Fig. 7g), while the meridional current velocities were slightly smaller, ranging from 0.1 to 0.12  $m \cdot s^{-1}$  southward (Fig. 7h). On the southern flank, currents were generally weaker (~0.1  $m \cdot s^{-1}$ ) and predominantly southward, whereas at the northern canyon flank, these were stronger (~0.2  $m \cdot s^{-1}$ ) and mainly oriented towards the southeast (Fig. 7i).

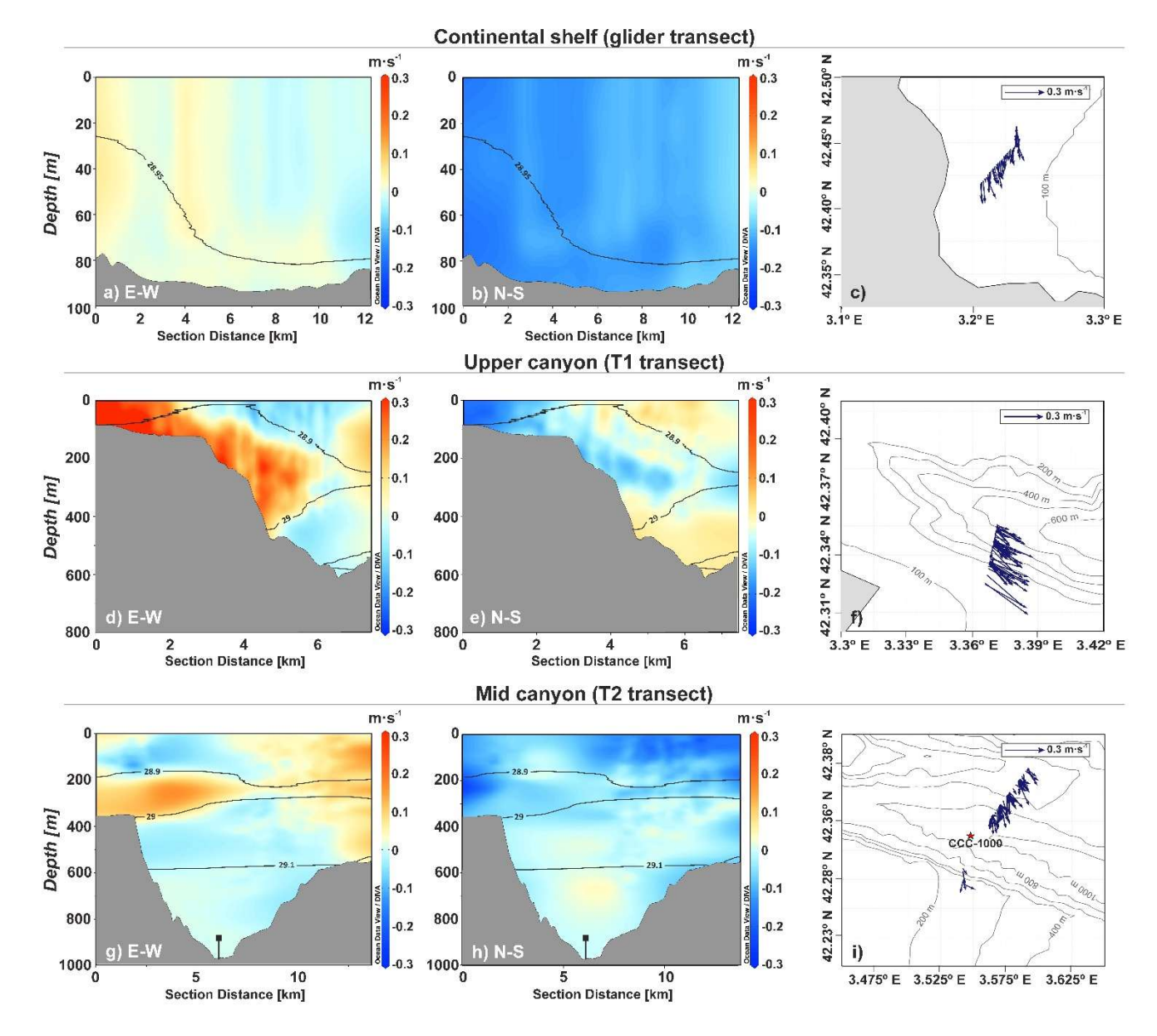


**Figure 7.** Contour plots of currents measured at (a-b) the continental shelf (glider transect) and at the Cap de Creus Canyon during (d-e) T1 transect and (g-h) T2 transect (FARDWO-CCC1 cruise). Eastward and northward current velocities are positive, while westward and southward current velocities are negative. Panels (c, f, and i) display stick plots representing the depth-averaged currents associated with dense waters for the three transects, defined between the 28.9 and 29.05 kg·m<sup>-3</sup> isopycnals.

#### 4.4. Duration and magnitude of DSWC during winter 2021-2022

The transports of dense shelf waters and associated SPM in the Cap de Creus Canyon during the observed MDSWC event in March 2022 were 0.7 Sv and 10<sup>5</sup> t across the continental shelf, 0.3 Sv and 10<sup>5</sup> t in the upper-canyon, and 0.05 Sv and 10<sup>4</sup> t in the mid-canyon. Since these observations provided only a snapshot of the event, we used the MedSea reanalysis product to extend our analysis and characterize the temporal evolution and magnitude of cascading events during winter 2021-2022. To do so, we first assessed the reliability of the MedSea by comparing it with our CTD observations (Fig. A1). In particular, we compared depth-averaged temperatures within the dense water plume (150-400 m depth) at stations where dense waters

were detected (Fig. A1), using the root mean square error (RMSE) statistical method. The RMSE were consistently low across all stations (< 0.2 °C) (Table 1), indicating a good agreement between both datasets. These results, along with the detailed validation presented in Fos et al. (2025), support the use of the MedSea reanalysis for studying DSWC in this region. In that study, the authors compared the MedSea output with long-term mooring data from the Cap de Creus and Lacaze-Duthiers canyons, and showed that, at 1000 m depth, the MedSea reproduces 84% of individual DSWC events within the same week and 56% on the exact date (Fos et al., 2025).

537

538

539

540

541

542

543

544

545

546

547

548

549

550

551

552

553

554

555

556

557

558

559

560

561

562

563

564

<u>Table 1.</u> Comparison of depth-averaged temperatures within the dense water plume derived from observations and reanalysis, with corresponding root mean square errors (RMSE). The location of CTD stations and reanalysis points is shown in Figure A1.

<b>Stations</b>	Observed temperature (°C)	Reanalysis temperature (°C)	RMSE (°C)
<u>T1-01</u>	12.41	<u>12.42</u>	<u>0.1</u> 6
<u>T1-02</u>	12.55	<u>12.4</u> 2	<u>0.1</u> 7
<u>T1-03</u>	12.34	12.42	<u>0.1</u> 8
<u>T1-04</u>	12.76	<u>12.4</u> 6	<u>0.2</u> 0
<u>T2-01</u>	<u>12.96</u>	<u>12.71</u>	<u>0.15</u>
<u>T2-02</u>	<u>12.68</u>	<u>12.65</u>	<u>0.0</u> 5
<u>T2-03</u>	12.72	<u>12.6</u> 5	<u>0.0</u> 7

Based on this validation, we used reanalysis to describe the temporal evolution and magnitude of dense water transports in the Cap de Creus Canyon. Daily MedSea reanalysis indicated that dense water transport was consistently higher in the upper-section than in the mid-canyon throughout winter (Fig. 8a), in agreement with observations. A significant increase in dense water down-canyon transport occurred in late January (> 0.2 Sv), coinciding with a drop in temperature (T < 12.9 °C) and a slight decrease in potential density to 28.85 kg·m<sup>-3</sup> (Fig. 8). Smaller transport (~0.12 Sv) was detected in the mid-canyon, but the time series of temperature do not seem to indicate the presence of dense shelf waters in the canyon at that depth (Fig. 9b). Four shallow cascading pulses were further identified in mid- and late February and early March, which had comparable down-canyon transport magnitudes (~0.2 Sv) in the upper canyon section (Fig. 8a). The strongest pulse, in mid-March, reached down-canyon transports of ~0.4 Sv in the upper canyon and ~0.1 Sv in the mid-canyon, accompanied by temperatures around 12 °C and potential densities ~28.9 kg·m<sup>-3</sup> (Fig. 8). Occasional up-canyon transports of lower magnitude (~0.1 Sv) were also detected (Fig. 8a), which likely reflect short-term current reversals along the canyon axis (not shown). As March progressed, dense water down-canyon transport gradually decreased, eventually ceasing in early April (Fig. 8a). Accordingly, the cascading season lasted approximately two months (from late January to mid-March), primarily affecting the upper canyon and with weaker influence further downcanyon. After the cascading season, transport shifted predominantly up-canyon (data not shown), reflecting the residual flux along the canyon axis, as previously reported for other canyons of the margin (Martín et al., 2006, 2007; Arjona-Camas et al., 2021).

Overall, the total volume of dense shelf waters transported during this period was estimated at 260 km<sup>3</sup> in the upper canyon and ~11 km<sup>3</sup> in the mid-canyon.

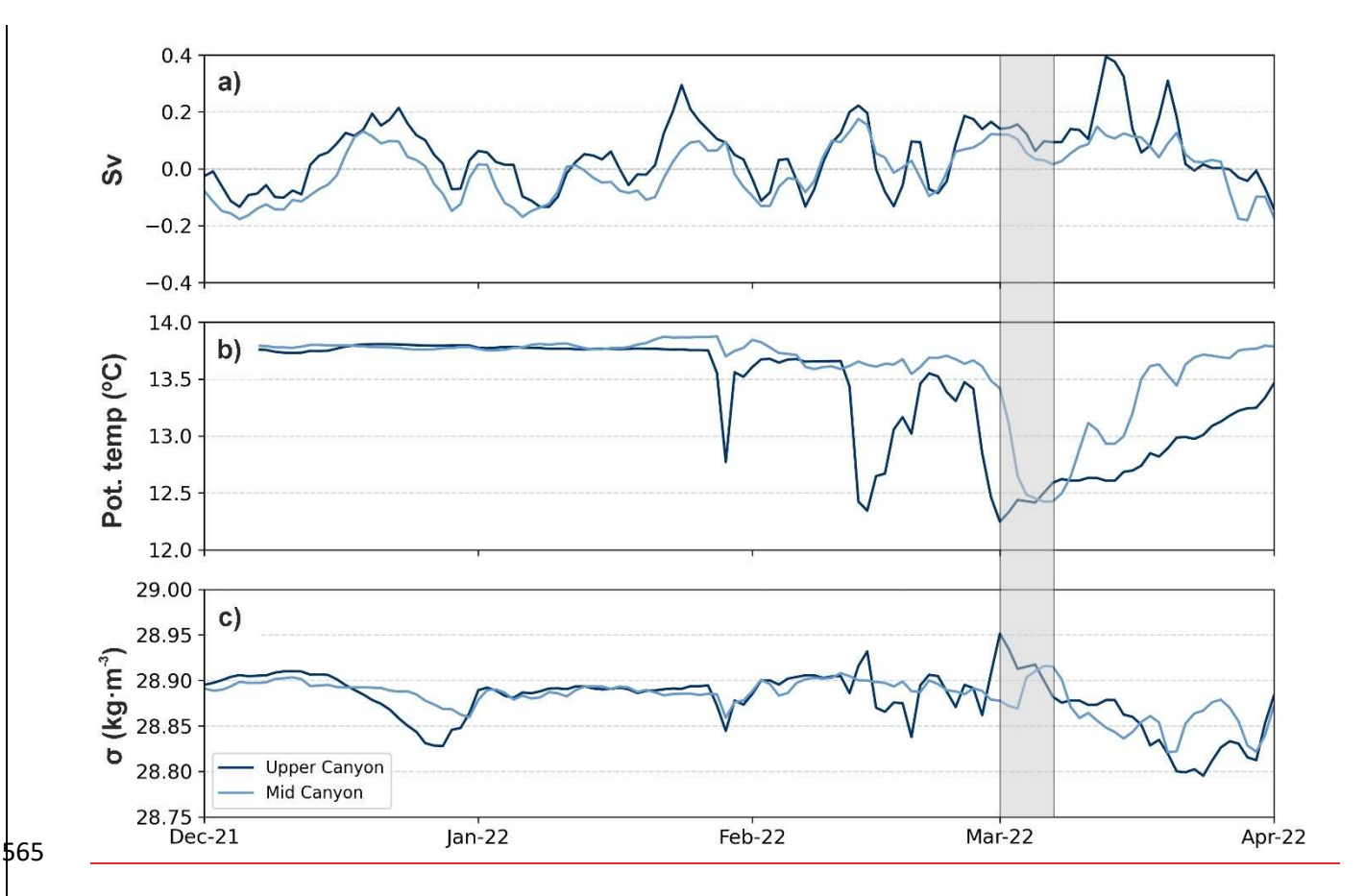


Figure 8. (a) Bathymetric map showing the location of T1 and T2 transects (green dots) conducted during the FARDWO CCC1 Cruise (March 2022). The two transects used to estimate the temporal variability of the along canyon transport at intermediate depths (350 m depth), located near T1 and T2, are also shown as coloured lines; (b-c) Time series of along-canyon transport (Sv) of dense waters, (b) potential temperature (°C), and (c) potential density (kg·m<sup>-3</sup>) for (in Sv) and its associated thermohaline characteristics (potential temperature, salinity, and potential density) for two transects: (b) the upper-canyon transect (blue line, near T1dark blue) and (c) the mid-canyon section (orange linelight blue), near T2), extracted from the Mediterranean Sea Physics Reanalysis product (Escudier et al., 2020; 2021). In panel (a), pPositive values in the first panels indicate down-canyon transport export, while negative values indicate up-canyon export. The grey shaded vertical bar highlights the FARDWO-CCC1 Cruise, which took place on March 1-7, 2022. transport.

#### 5. Discussion

78

79

# 5.1. Forcing conditions during winter 2021-2022 Forcing conditions during winter 2021-2022

The winter of 2021-2022 was characterized by two distinct periods: an early winter (December-January) first typical winter phase from December to January with several short northerly and northwesterly windstorms that caused continuous heat losses in the GoL, followed by a late winter (second period from February to March) dominated by marine eastern storms and lower heat losses (Figs. 3a-c). During the first period, the averaged sea atmosphere heat loss was around 158 W·m² (Fig. 3a). In contrast, the second period showed reduced mean heat losses (-70 W·m²) (Fig. 3a). Overall, The mean averaged sea atmosphere heat loss over the season for the whole winter-was -150 W·m² (Fig. 3a), 25% lower than typical mild winters in the GoL (-200 W·m²) and half the magnitude of severe winters such as 2004-2005 slightly lower than typical mild winters in the GoL (-200 W·m²) and much lower than severe winters such as 2004-2005 (-300 W·m²) (Schroeder et al., 2010). From late November to February, several short but intense episodes of heat loss (~400 W·m²) were recorded, peaking in January

Despite this, intense short episodes of heat loss (-500 W·m<sup>-2</sup>) occurred in January 2022 (-500 W·m<sup>-2</sup>) (Fig. 3a), which which likely contributed to significant surface water cooling and buoyancy loss, especially on the inner shelf (Figs. 3e-g). Water Shelf water temperatures dropped below 12.9 °C in late December/early January and below 12 °C in mid/late February (Fig. 3e), while shelf water density-densities increased to 28.9-28.95 kg·m<sup>-3</sup>, exceeding the pre-winter maximum of 27.9 kg·m<sup>-3</sup> (Fig. 8a9a). This-These conditions allowed shelf waters formed over the GoL's shelf to spread as a near-bottom layer across the mid and outer shelf and cascade downslope (Figs. 3 and 8b9b, c). This likely marked the beginning of the MDSWC period, a scenario consistent with previous studies in the GoL (Dufau-Julliand et al., 2004; Durrieu de Madron et al., 2005; Canals et al., 2006; Ulses et al., 2008a).

The cyclonic circulation on the western part of the shelf, driven by the prevailing northerly winds (Ulses et al., 2008a; Bourrin et al., 2008), promoted the transport of these dense shelf waters along the coast (Fig. 9b). The narrowing of the shelf near the Cap de Creus Peninsula further accelerated their overflow into the upper slope, mainly cascading into the westernmost canyons (i.e., Lacaze-Duthiers and Cap de Creus Canyons) (Figs. 9b, c) (Ulses et al., 2008a). According to the MedSea reanalysis, the first cascading pulse in the Cap de Creus Canyon occurred in late January, coinciding with the arrival of cold, dense shelf waters into the upper canyon (Fig. 8). During late winter, especially from late February to late March, four additional cascading pulses occurred in the canyon, the strongest in mid-March (Fig. 8a). This event was strengthened by an eastern storm, which likely enhanced DSWC into the canyon. The role of eastern storms in enhancing DSWC events has been previously documented for the Cap de Creus Canyon in similar studies in the GoL (e.g., Palanques et al., 2008; Ogston et al., 2008; Ribó et al., 2011). Throughout this period, these windstorms were often accompanied with increased freshwater discharge of coastal rivers (Fig. 3d). Such freshwater inputs are commonly observed during mild winters in the region and can locally reduce salinity and density over the shelf (Ulses et al., 2008a; Martín et al., 2013; Mikolajczak et al., 2020), but appeared to have limited impact on shelf water densification during the studied winter (Fig. 3e).

Overall, the mild atmospheric conditions during winter 2021-2022 limited the downslope transport of dense waters into the deeper canyon sections (Fig. 4). As a result, the mild winter of 2021-2022 only generated shallow cascading into the Cap de Creus Canyon (Figs. 5 and 6). The MedSea reanalysis further confirmed that dense water transport was consistently higher in the upper canyon than in the mid canyon (Fig. 9a).

mild

\$87

\$88

\$89

590

\$91

592

593

**\$**94

\$95

\$96

\$97

598

**5**99

600

601

602

603

604

605

606

607

608

609

610

611612613

614

TFigs. 8b, c) (

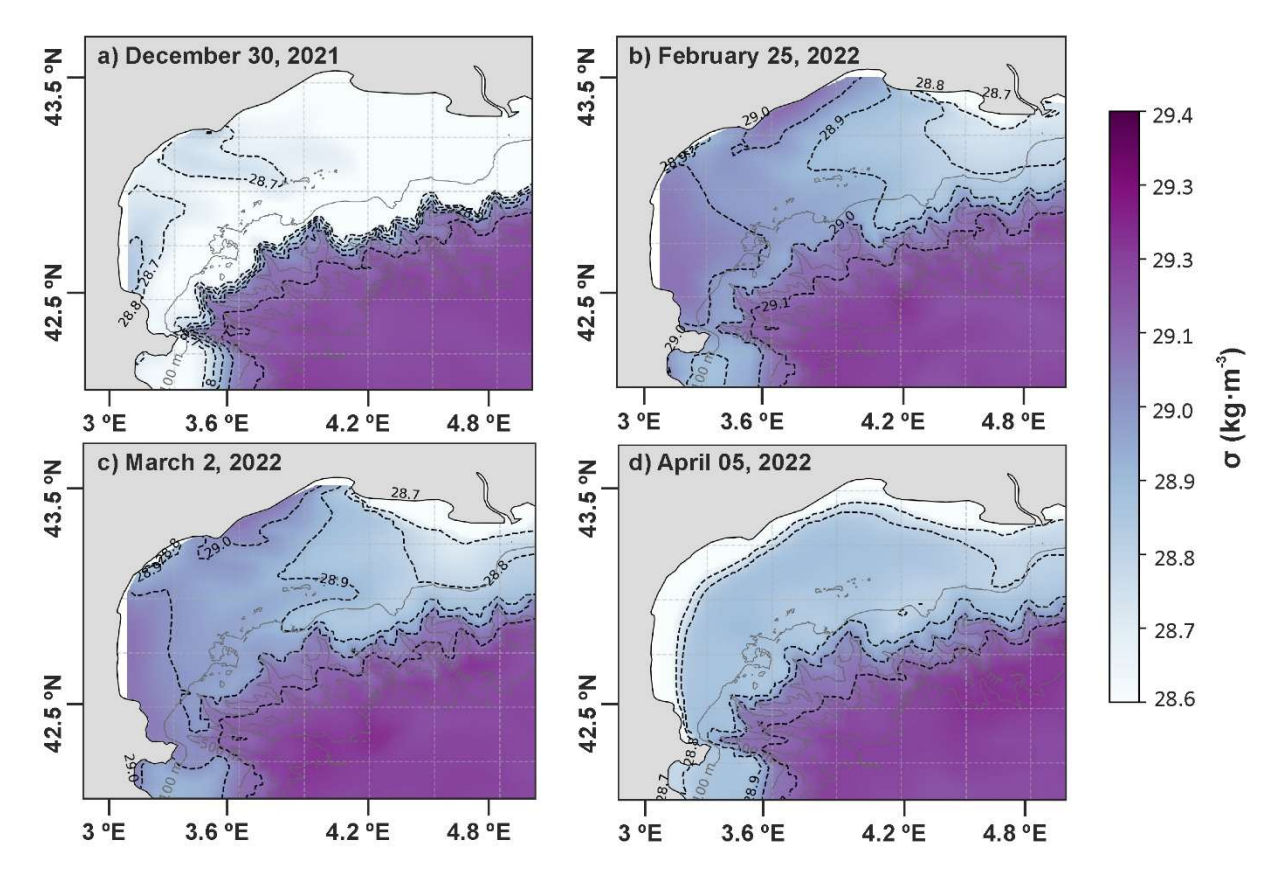


**Figure 28.** Bathymetric maps of the Gulf of Lion (GoL) showing the potential density anomaly at bottom for four days during the winter of 2021-2022: (a) December 30, 2021; (b) February 25, 2022; (c) March 2, 2022; and (d) April 5, 2022. Density contours (black) are displayed every 0.1 kg·m<sup>-3</sup>. Data has been obtained from the Mediterranean Sea Physics Reanalysis product (Escudier et al., 2020; 2021).

# 5.2. DSWC in the Cap de Creus Canyon in March 2022

615 **6**16

617

618

619

620 621

622

623

624

625

626

627

628

629

630

631

632

633

634

635

636

637

638

During the observational period in early March 2022, one of the shallow cascading pulses previously identified in the MedSea reanalysis (Fig. 8) was directly monitored over the narrow continental shelf and within the Cap de Creus Canyon (Figs. 5-7). DMoreover, during winter, especially throughout February and March 2022, the region was impacted by several easterly/southeasterly windstorms, often associated with increased freshwater discharge from the Rhône River and the coastal rivers (Fig. 3d). Such freshwater inputs are commonly observed during mild winters in the region and can locally reduce salinity and density over the shelf (Ulses et al., 2008a; Martín et al., 2013; Mikolajezak et al., 2020). In contrast, winters favorable to IDSWC, such as 2004 2005, 2005 2006, and 2011 2012, are marked by stronger heat losses, sustained cooling and notably low river discharge (Ulses et al., 2008b). For example, during winter 2004 2005, the Rhône River discharge averaged only ~1400 m<sup>3</sup>·s<sup>-1</sup> between December and March, which is below the mean annual discharge (1920-2007) of 1850 m<sup>3</sup>-s<sup>-1</sup> (Pont et al., 2002; Provansal et al., 2014). These conditions allowed shelf waters to gain potential densities exceeding 29.1 kg·m<sup>-3</sup>, which are sufficient to break through the Eastern Intermediate Water (EIW) layer and generate deep cascading, even reaching depths > 2000 m (Font et al., 2007; Durrieu de Madron, 2013; Palanques and Puig, 2018). Contrary, during the mild winter of 2021-2022, although winter cooling led to shelf water densification (~28.95 kg·m<sup>-3</sup>), dense waters were not dense enough to overcome the EIW and reach the deep basin. Instead, they spread along the mid shelf and upper slope (Fig. 8b, c). The cyclonic circulation on the western part of the shelf, driven by the prevailing winds (Ulses et al., 2008a; Bourrin et al., 2008), promoted the transport of these dense shelf waters along the coast (Fig. 7b). The narrowing of the shelf near the

Cap de Creus Peninsula further accelerated the overflow of dense shelf waters into the upper slope, mainly caseading into the westernmost canyons (i.e., Lacaze Duthiers and Cap de Creus Canyons) (Ulses et al., 2008a).

Nevertheless, the mild atmospheric conditions during winter 2021–2022 prevented the transport of dense waters into the deeper sections of these canyons. In fact, the mooring data acquired in the Lacaze Duthiers and Cap de Creus canyons clearly indicate that dense shelf waters did not reach the deeper canyon sections during that winter. In both moorings, the recorded current speeds remained below 0.2 m·s<sup>-1</sup>, temperatures were nearly constant (13.5 °C), and SPM concentrations were <1 mg·L<sup>-1</sup> (Fig. 4), indicating the absence of a deep cascading. For IDSWC events, previous mooring data have registered much colder near-bottom temperatures (11-12.7 °C), stronger down-canyon velocities (> 0.8 m·s<sup>-1</sup>), and significantly higher SPM concentrations (~40 mg·L<sup>-1</sup>) (Canals et al., 2006)., prevented a significant increase in the density of shelf waters (Herrman et al., 2008; Mikolajezak et al., 2020). This limitation, in turn, restricted the intrusion of dense shelf waters into deeper sections of the slope and the westernmost canyons, including the Lacaze Duthiers and the Cap de Creus Canyons (Fig. 4g).

5.2. Dense shelf water cascading event in the Cap de Creus CanyonIn early March 2022, during the glider survey, the presence of dense shelf waters (T < 12.9 °C and S < 38.4) was were detected at over the narrow continental shelf adjacent to the head of the Cap de Creus Canyon\_(Figs. 5a-c). The steep bathymetry of the inner shelf, combined with the prevailing southwestward currents, facilitated the cascading of dense shelf waters into the canyon head (Dufau-Julliand et al., 2004; Canals et al., 2006; DeGeest et al., 2008). Previous works have demonstrated that, once dense shelf waters reach the Cap de Creus Peninsula, they are deflected and start to pool the outer shelf until they spill into the Cap de Creus Canyon from the southern flank (Dufau Julliand et al., 2004; Canals et al., 2006; DeGeest et al., 2008).

The relatively steep bathymetry of the inner shelf, combined with the prevailing southeastward currents (Figs. 7a e), facilitated the transport of dense waters into the upper section of the Cap de Creus Canyon. Most likely, these dense waters were pushed into the canyon by cascading currents or storm induced downwelling processes associated with northerly/northwesterly winds (Fig. 3b), as previously documented for the mild winter of 2010-2011 (Martín et al., 2013). Within In the upper canyon section, dense waters were the T1 transect showed a vein of cold, fresher water, rich in oxygen and chlorophyll-a observed between 100 and 400 m depth (core depth: 380 m) (Figs. 5d-f and 6d-f), detaching above the EIW (~400 m depth) (Fig. A1) and . This flow traced the export of a vein of coastal dense waters exported from the shelf towards the upper continental slope, which contributed contributing to the body of WIW (Figs. 5d-f, 6d-f, and B1Figs. 5d-f and A1). During this cascading event, The WIW likely formed on the outer shelf of the GoL during winter through intense surface cooling and convective mixing of the AW, and then advected southward to the Cap de Creus Canyon by the general circulation (Lapouyade and Durrieu de Madron, 2001; Dufau-Julliand et al., 2004; Juza et al., 2019), the dense water plume continued flowing downcanyon to the mid canyon (Figs. 7d-f), where it detached from the southern flank between 250 and 380 m depth and further contributed to the WIW body (Figs. 5g-i). The WIW was likely formed on the outer shelf of the GoL during winter through intense surface cooling and convective mixing of the AW, and then advected southward to the Cap de Creus Canyon by the general circulation (Lapouyade and Durrieu de Madron, 2001; Dufau-Julliand et al., 2004; Juza et al., 2019). Based on the observations during this shallow cascading event, it is plausible that the other events detected in the canyon during this mild winter shared similar characteristics, with dense waters confined to the upper canyon and contributing to the WIW body.

At the mid-canyon, dense waters shifted to a more southward direction compared to the predominantly southeastward direction in the upper canyon (Figs. 7f, i). This flow shift suggests that, as the canyon topography opens, dense waters were no longer constrained by the canyon and veered southward, following the continental slope (Millot, 1990). Previous studies have shown that part of these waters can continue flowing across the Gulf of Roses and reach the neighbouring Palamós and Blanes Canyons (Zúñiga et al., 2009; Ribó et al., 2011). This advection is facilitated by the presence of a shallow NNE-SSW oriented channel that extends from the narrow shelf of the Cap de Creus Canyon to the head of the Palamós Canyon (Durán et al., 2014). During the observed MDSWC event, dense shelf waters and the WIW were likely advected southward through this

channel, eventually reaching neighbouring canyons, as documented in previous mild winters (e.g., Arjona-Camas et al., 2021). This southward advection most likely occurred during the other cascading pulses detected in the reanalysis for the studied winter.

In contrast, -during extreme winters, dense waters reach potential densities exceeding that of the EIW, generating deep cascading that transports them all the way down canyon (Font et al., 2007; Durrieu de Madron et al., 2013; Palanques and Puig, 2018), rather than following the southward along-slope routes characteristic of MDSWC events.

# 5.3. Suspended sediment transport during MDSWC events in the Cap de Creus Canyon

 During the observational period in early March 2022, MDSWC acted as a pathway to transport SPM and chlorophyll across the continental shelf into the Cap de Creus Canyon (Figs. 5 and 6). Riverine inputs from the Rhône and smaller coastal rivers were low prior to the cruise (Fig. 3d), suggesting that they did not contribute significantly to the increased SPM observed during the event. Conversely, storm-waves and cascading-induced currents were likely the main mechanisms of sediment resuspension and transport. This is consistent with previous findings by Estournel et al. (2023), who documented that, during the mild winter of 2010-2011, storm-induced currents remobilized shelf sediments that subsequently fed the upper section of the Cap de Creus Canyon and along the North Catalan shelf.

Increased SPM and chlorophyll values were mainly observed along the southern canyon flank in both the upper and mid canyon, which suggests that dense shelf waters transported phytoplankton cells and contributed additional organic particles to the canyon (Figs. 6d-i). Phytoplankton blooms, which typically peak between December and January, likely provided newly produced biological particles to GoL shelf waters, further enhancing the transport of organic matter into the canyon during this MDSWC event (Fig. B1; Fabres et al., 2008). The preferential accumulation of SPM along the southern canyon flank, contrasting with clear waters on the northern canyon flank, can be explained by the canyon's asymmetric morphology and hydrodynamics. The very narrow adjacent shelf (2.5 km) brings the southern canyon rim close to the coast (Lastras et al., 2007; Durán et al., 2014), where a coastal eddy near the Cap de Creus Peninsula steers dense shelf waters and associated SPM towards the southern flank (Davies et al., 1995; DeGeest et al., 2008). The asymmetric canyon walls reflect this preferential pathway: the northern flank is relatively smooth, with fine-grained silty clays and relatively high accumulation rates (up to 4.1 mm·yr<sup>-1</sup>), indicative of a depositional area. On the other hand, the southern flank has erosional features, coarser sediments such as gravel, lower accumulation rates (~0.5 mm·yr<sup>-1</sup>), and oblique furrows interpreted as signatures of DSWC events (Canals et al., 2006; Lastras et al., 2007; DeGeest et al., 2008).

If we examine the hydrodynamics of the dense water plume, it exhibits characteristics consistent with the "head up" configuration described in Shapiro and Hill (2003), in which most of the dense water remains upslope while only a thin tail extends downslope. This configuration suggests a limited downslope export of dense waters. To further characterize the flow regime of the plume, we estimated two dimensionless numbers: the Richardson number (Ri) and the Froude number (Fr), both of which provide insights into the stability and dynamical behaviour of stratified flows.

The Ri is a ratio between the Brünt-Väisäla frequency squared (N²) and the vertical shear of the horizontal velocity (S²), and describes the tendency of a stratified flow to remain laminar or become turbulent (Monin and Yaglom, 1971). For this calculation, we used temperature, salinity, and E W current velocities from CTD and LADCP measurements acquired during the cruise. Ri values showed a general increase between 150 and 300 m depth, which roughly corresponds to the vertical extent of the dense shelf water plume (Fig. C1). The maximum Ri observed reached 0.18 at 270 m depth in the upper canyon, and 0.16 at 180 m in the mid canyon. These values are below the critical threshold of 1 that separates laminar (Ri >1) from turbulent flow regimes, thus indicating a predominantly turbulent flow (Mack and Schoeberlein, 2004). This suggests that fluid instabilities likely enhanced vertical mixing and lateral spreading of the dense water plume.

Complementary, we estimated the Froude number  $(Fr = U/\sqrt{g'h})$ , following the approach by Cenedese et al. (2004), which distinguishes between laminar, wavy, and eddying flow regimes in dense bottom currents over slopes. Using a

representative current velocity (U) of 0.18 m·s<sup>-1</sup>, a dense layer thickness (h) of 100 m, and a reduced gravity (g') of 2.67·10<sup>-4</sup> m·s<sup>-2</sup>, we obtained Fr ~1.10. This value lies just above the critical threshold of 1, indicating a supercritical flow regime where inertial forces become more significant, potentially favoring more unsteady and turbulent flow conditions (Cenedese et al., 2004).

Within the Cap de Creus Canyon, coastal dense shelf waters flowed predominantly along the southern canyon flank, associated with increased SPM concentrations (Figs. 6 and 7). This suggests that during this MDSWC event, dense waters transported sediment particles into the canyon down to intermediate depths (Fig. 6d). The time series of water discharge from the Rhône River and the smaller coastal rivers does not seem to indicate important freshwaters and sediment inputs prior to the cruise (Fig. 3d). In fact, both the Rhône River and the coastal rivers had relatively low discharges before the cruise (Fig. 3d). This points to storm waves and cascading induced currents, rather than riverine input, as the main mechanisms of sediment resuspension and transport. This is consistent with previous findings by Estournel et al. (2023), who described that, during the mild winter of 2010-2011, storm induced downwelling events contributed to the remobilization of shelf sediments that fed the upper section of the Cap de Creus Canyon and along the North Catalan shelf. In fact, during mild winters, most of the sediment delivered by the GoL's rivers remains relatively close to their mouths after floods and it is later remobilized by storm waves under highly energetic conditions (Guillén et al., 2006; Estournel et al., 2023). In addition, the increased fluorescence values observed within the dense water plume suggests the mixing of terrestrial sediments with phytoplankton cells (Figs. 6e, h). Phytoplankton blooms, which typically peak between December and January, likely contributed newly produced biological particles to GoL's shelf waters, thereby enhancing the transport of organic matter into the canyon during the observed MDSWC event (Fig. B1; Fabres et al., 2008).

The dense water plume continued flowing down canyon to the mid canyon section, where it contributed to the WIW body that extended to depths of 380 m (Figs. 5g i). At these depths, enhanced SPM concentrations were observed on the southern flank, contrasting with clear waters on the northern canyon flank (Fig. 6g). The contrast in SPM concentrations between the flanks of the Cap de Creus Canyon actually reflects its marked asymmetric morphology and hydrodynamics. One key aspect is the very narrow adjacent shelf (2.5 km), which brings the southern rim of the canyon into close proximity with the coast (Lastras et al., 2007; Durán et al., 2014). The canyon itself presents very dissymmetric walls: the northern canyon wall is relatively smooth, with fine-grained silty clays and relatively high accumulation rates (up to 4.1 mm·yr<sup>-1</sup>), indicative of a depositional area. On the other hand, the southern flank has erosional features (exposed bedrocks and gullies), and coarser sediments such as gravel. These characteristics, along with lower accumulation rates (~0.5 mm·yr<sup>-1</sup>), suggest active sediment transport and bypassing processes (Lastras et al., 2007; DeGeest et al., 2008). In addition, other studies have evidenced the presence of furrows oblique to the canyon axis, which have been interpreted as signatures of DSWC events over the southern canyon wall (Canals et al., 2006). This has been later confirmed through modeling and observations (DeGeest et al., 2008), which also identified episodic strong currents in the southern canyon rim during cascading events in this area. Furthermore, the conceptual model proposed by DeGeest et al. (2008) suggest that the coastal current forms an eddy over southwestern shelf near the Cap de Creus headland (Davies et al., 1995), which likely steers dense water flows and sediment preferentially toward the southern canyon rim (DeGeest et al., 2008). Altogether, these morphological and hydrodynamic features likely offer a plausible explanation explain for the enhanced SPM concentrations observed along the southern canyon wall in both upperand mid-canyon sections during our the observed MDSWC eventstudy (Figs. 6d, g).

Although direct observations were limited to the early March event, the other cascading pulses detected in the MedSea reanalysis for the same winter probably exhibited similar SPM transport dynamics. During these events, dense shelf waters would have transported SPM along the southern canyon flank to the upper canyon, or exported them southward along the coast. Such behavior resembles transport patterns reported for previous mild winters (Martín et al., 2013; Estournel et al., 2023). Nevertheless, during the mid-March storm, coastal rivers exhibited a peak in discharge (Fig. 3d), which may have locally enhanced sediment delivery to the canyon, transporting additional SPM during this cascading event.

Overall, it is plausible that the other shallow cascading pulses transported comparable amounts of dense waters and sediments to the canyon, although these estimates remain uncertain due to the lack of direct measurements.

Our data also show that dense waters along the southern canyon flank shifted from a predominantly southeastward direction in the upper canyon section to a more southward direction in the mid canyon section (Figs. 7f, i). This transition suggests that, as the canyon topography opens, dense waters are no longer confined by its walls and begin to veer southward, following the continental slope (Millot, 1990). Previous studies have shown that part of these waters can continue flowing southward crossing the Gulf of Roses and reaching the neighbouring Palamós and Blanes Canyons (Zúñiga et al., 2009; Ribó et al., 2011). This is supported by the presence of a shallow NNE-SSW oriented channel that extends from the narrow shelf of the Cap de Creus Canyon to the head of the Palamós Canyon (Durán et al., 2014). During MDSWC events, this channel facilitates the along slope transport of dense waters (particularly WIW) and associated suspended sediment towards the Palamós Canyon (Ribó et al., 2011; Martín et al., 2013). A similar mechanism may have occurred during the studied winter here (2021-2022), when WIW could have been advected southward through this channel and eventually reached neighbouring canyons, as previously documented during the winter of 2017 (Arjona Camas et al., 2021).

In fact, during the studied winter, although winter cooling led to shelf water densification (~28.95 kg·m³), dense waters were not dense enough to overcome the EIW and reach the deep basin, as opposed to IDSWC events during extreme winters, potential densities exceeding 29.1 kg·m³, which are sufficient to break through the Eastern Intermediate Water (EIW) layer and generate deep cascading, even reaching depths > 2000 m (Font et al., 2007; Durrieu de Madron et al., 2013; Palanques and Puig, 2018).

#### 5.3. Spatial and temporal variabiliaty of dense shelf water export in the Cap de Creus Canyon

#### 5.4. Interannual variability of dense shelf water transports and future perspectives of DSWC

DSWC in the GoL shows strong interannual variability mainly related to the magnitude and timing of atmospheric forcings (surface heat losses), which ultimately control shelf water densification and, consequently, the magnitude of cascading events, even during mild winters (Herrmann et al., 2008; Mikolajczak et al., 2020). For instance, dense water transports during the mild winters of 2003-2004, 2010-2011, and 2021-2022 were ~75 km<sup>3</sup>, ~1500 km<sup>3</sup>, and ~260 km<sup>3</sup>, respectively, partly reflecting the different net heat losses in those winters (-125 W·m<sup>-2</sup> in 2003-2004, -200 W·m<sup>-2</sup> in 2010-2011, and -150 W·m<sup>-2</sup> in 2021-2022) (Herrmann et al., 2008; Ulses et al., 2008a; Mikolajczak et al., 2020). During 2003-2004 and 2010-2011, shelf water densities (~27.78-28.8 kg·m<sup>-3</sup>) were insufficient to generate cascading beyond ~300-350 m depth and contributed little to the WIW body in the canyon (Ulses et al., 2008a; Martín et al., 2013). In these winters, dense waters did not cascade offshelf, but merely downwelled into the canyon induced by the strong cyclonic circulation during eastern storms and by the subsequent accumulation of seawater along the coast (Martín et al., 2013; Rumín-Caparrós et al., 2013; Mikolajczak et al., 2020). In contrast, in winter 2021-2022, shelf waters reached slightly higher densities (~28.8-29.1 kg·m<sup>-3</sup>), cascading further downslope in the upper canyon down to ~400 m depth and contributing to the WIW body (Figs. 5 and B1). Nevertheless, downwelling at the canyon head in winter 2010-2011 reached daily magnitudes (~0.2 Sv and 10<sup>5</sup> t of SPM; Martín et al., 2013) comparable to the transports during the MDSWC event observed in March 2022. Overall, this illustrates that the intensity and magnitude of DSWC, as well as associated transports, can vary even during mild winters with similar atmospheric characteristics. In comparison, the extreme winter of 2004-2005 was associated with much stronger net heat losses (~-300 W·m<sup>-2</sup>) that led to the formation of very dense shelf waters (>29.1 kg·m<sup>-3</sup>) and IDSWC into the deep basin (Canals et al., 2006; Palanques et al., 2006; Ulses et al., 2008a, b; Puig et al., 2013). The total dense water transport during this extreme event was considerably higher than during mild winters, reaching values ~1640 km<sup>3</sup> (Ulses et al., 2008a). The winters of 2005-2006 and

2011-2012 were also classified as extreme, reflecting similarly strong heat losses and IDSWC events (Palanques et al., 2012; Durrieu de Madron et al., 2013).

Over the past two decades, dense water transport through the Cap de Creus Canyon has shown considerable variability across mild and extreme winters (Fig. 10). According to Mikolajczak et al. (2020), mild winters from the warmest to coldest were 2016-2017, 2010-2011, 2013-2014, and 2015-2016, with the two warmest years presenting the largest numbers of easterly winds (10-11 days) and, consequently, enhanced dense water transports (Fig. 10). Reanalysis data during winters 2010-2011 and 2016- 2017 showed dense waters transports between 0.2-0.4 Sv (Fig. 10). The winter of 2021-2022 experienced 14 days of easterlies, but considering dense water transport, the magnitude of heat losses, and other forcing factors, it would fall between the 2016-2017 and 2010-2011 winters. In contrast, IDSWC events have occurred less frequently, typically every 5-7 years and often in pairs (Fig. 10), and are generally associated with higher dense water transports than MDSWC events, and fewer days of easterlies (~1 day). Extreme winters (from the coldest to the warmest: 2004-2005, 2005-2006, 2011-2012, 2012-2013) (Mikolajczak et al., 2020) showed transports ranging from ~0.3 to 0.6 Sv, with the strongest transports occurring in 2004-2005 and 2005-2006 (~0.6 Sv), and lower in 2011-2012 (~0.3 Sv) and 2012-2013 (~0.4 Sv) (Fig. 10). The interannual variability of IDSWC events is likely controlled by intense atmospheric forcing during cold winters, although the precise mechanisms that trigger these events need further analysis (Fos et al., 2025).

However, as shown by the reanalysis time series (Fig. 10) and recent numerical simulations (Mikolajczak et al., 2020), mild and extreme winters can sometimes reach similar magnitudes of dense water transport despite having contrasting atmospheric conditions. For example, during the mild winter of 2010-2011, the total dense water export (1500 km³) was comparable to the extreme winter of 2004-2005 (1640 km³), but the preferential pathways differed. In winter 2010-2011, only 30% of the transport occurred through the canyon, while 70% followed along the coast or remained around the upper canyon. In winter 2004-2005, 69% of dense shelf water cascaded through the Cap de Creus Canyon down to the deeper parts of the canyon (Ulses et al., 2008a; Mikolajczak et al., 2020). It is very likely that during the winter of 2021-2022, a high proportion of dense waters and associated SPM followed along the coast or southward along the upper slope and canyon. In addition, these findings suggest that during mild winters, MDSWC events may primarily influence coastal ecosystems, whereas during extreme winters, IDSWC may significantly impact deep-benthic ecosystems (Mikolajczak et al., 2020).

Over the past two decades, MDSWC events have been the most common form of dense shelf water export through the Cap de Creus Canyon, as reported in previous studies (Herrmann et al., 2008; Durrieu de Madron et al., 2023), and as further evidenced by the time series of dense water transport estimated from reanalysis data shown in Figure 10. In contrast, IDSWC events have occurred less frequently, typically every 5-7 years, and are often associated with higher transports of dense shelf waters (Fig. 10).

Putting the winter 2021-2022 into perspective, the total dense water transport (260 km³) was approximately half of the total volume simulated for the mild winter of 1998-1999 (500 km³) (Dufau-Julliand et al., 2004), and higher than the total export estimated for the mild winter of 2003-2004 (75 km³) (Ulses et al., 2008a). Compared to the extreme IDSWC event of 2004-2005, one of the most studied events in the GoL, the 2021-2022 MDSWC event accounted for roughly half of the total dense water volume exported through the Cap de Creus Canyon (> 750 km³) (Canals et al., 2006; Ulses et al., 2008b). However, as shown in the reanalysis time series (Fig. 10) and recent numerical simulations (Mikolajczak et al., 2020), mild and extreme winters can sometimes reach similar magnitudes of dense water export despite having contrasting atmospheric conditions. For example, during the mild winter of 2010-2011, the total dense water export (1500 km³) was comparable to the extreme winter of 2004-2005 (1640 km³) (Ulses et al., 2008a). The key difference lies in the preferential export pathways: in 2004-2005, 69%

**\$**74

75

. 

**\$**79

of dense shelf water easeaded through the Cap de Creus Canyon down to the deeper parts of the eanyon. In contrast, in winter 2010-2011, only 30% of the export occurred through the canyon, while 70% followed along the coast or remained around the upper canyon section (Ulses et al., 2008a; Mikolajezak et al., 2020). This difference may also affect the distribution of suspended sediment, which instead of being advected to deeper canyon areas, is likely redistributed along the shelf or accumulates in the upper canyon. Based on our results, it is very likely that during the winter of 2021-2022, a higher proportion of dense waters and associated suspended sediment was exported along the coast or only generated shallow cascading into the upper canyon, resembling the export pattern observed during the mild winter of 2010-2011. These findings suggest that during mild winters, MDSWC events may primarily influence coastal ecosystems, whereas in extreme winters, IDSWC may significantly impact deep benthic ecosystems (Mikolajezak et al., 2020).

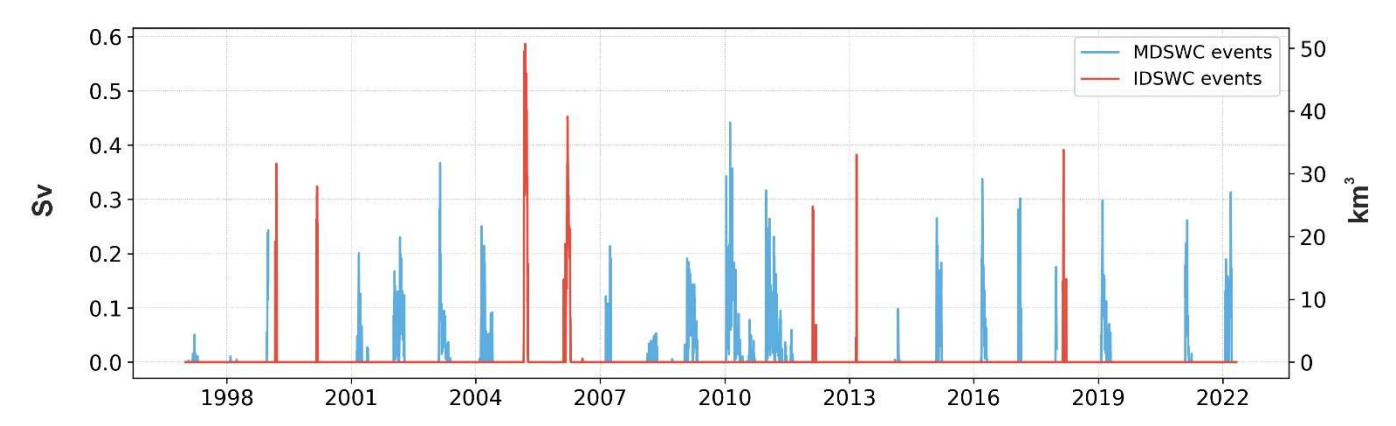


**Figure 10.** Interannual variability Time series of daily down-canyon transport of dense shelf waters (Sv) from 1997 to 2022, calculated across a central transect in the upper region of the Cap de Creus Canyon (see location in Figure 1). The occurrence and magnitude of IDSWC events, defined by densities > 29.1 kg·m<sup>-3</sup>, is are highlighted in red, whereas mild events, with densities below this threshold, are highlighted in blue. Data have been extracted from the Mediterranean Sea Physics Reanalysis product (Escudier et al., 2020; 2021).

Future climate projections indicate an increasing frequency of mild winters in the northwestern Mediterranean (Herrmann et al., 2008; Durrieu de Madron et al., 2023). Under the IPCC-A2 scenario, DSWC could decline by 90 % at the end of the 21<sup>st</sup> century (Herrmann et al., 2008). This scenario would drastically reduce both the intensity and depth penetration of DSWC.

Recent studies have already pointed out to a warming and salinification of surface and intermediate waters across the northwestern Mediterranean (Margirier et al., 2020), which would increase the stratification of the water column and hinder deep-ocean convection. Such reduction could strengthen the production of WIW by favouring intermediate-water formation over deep-water ventilation (Parras-Berrocal et al., 2022). Consequently, dense shelf water transport could become more limited to near-coastal areas or upper-canyon regions, altering the regional hydrology and impacting the Mediterranean Thermohaline Circulation (Somot et al., 2006).

Ongoing sea warming and increasing stratification are also expected to impact shelf-slope exchanges, reducing IDSWC activity and the associated SPM transports of particulate matter from the GoL to the deep basin (Somot et al., 2006). As a result, the transfer of dense shelf waters and organic matter to the deep sea would be confined to the Catalan shelf or upper Cap de Creus Canyon (Estournel et al., 2023). drastically reduced and mainly redirected along the Catalan shelf or the upper reaches of the Cap de Creus Canyon (Estournel et al., 2023). A decline in the frequency of marine storms could also promote sediment retention in the Rhône River prodelta, reducing the transfer of particulate matter towards the slope and deep basin (Estournel et al., 2023). These changes could significantly alter-modify transport pathways and affect erosion and

deposition patterns along the incised submarine canyons of the GoL, and in consequence, have important impacts in deep benthic communities that rely on the arrival of suspended particulate matter. Cold water corals, benthic invertebrates, and commercially important species such as shrimps may be particularly vulnerable, as the limited supply of nutrients and oxygen would hinder their survival (Puig et al., 2001; Pusceddu et al., 2013). In Lacaze-Duthiers Canyon, for instance, Chapron et al. (2020) showed that cold-water coral growth is strongly influenced by the intensity of DSWC events, which modulate their feeding conditions and development. Intense-IDSWC events cause high budding rates but low colony linear extension by limiting prey capture rates with high current speeds, whereas -Mild-MDSWC events cause both high budding rates and high linear extension associated with enhanced higher organic matter supply. In contrastConversely, the absence of easeading plumes-DSWC events can cause high mortality (Chapron et al., 2020). Regardless of the direction of DSWC's effects on deep-sea ecosystems, it has been demonstrated that even a small loss of biodiversity can lead to a major ecosystem collapse (Danovaro et al., 2008), with cascading impacts on ecosystem services such as fisheries (Pörtner and Knust, 2007; Smith et al., 2009).

#### 6. Conclusions

17

19

This paper provides a comprehensive observational characterization of a MDSWC event shelf slope exchanges of dense shelf waters and associated SPM transport in the Cap de Creus Canyon during during athe mild winter of 2021-2022 MDSWC event. We combined study used a multiplatform approach, combining data from glider datas, ship-based CTD transects, instrumented mooring lines, and reanalysis products data to assess investigate both the spatial and temporal evolution of shelf-to-canyon transports of dense waters and SPM. dense water and sediment dense shelf water and associated sediment transport export in the Cap de Creus Canyon during the mild winter of 2021-2022.

The first part of the winter 2021-2022 (December and January) The winter of 2021-2022 was characterized dominated by several days of northerly and north-westerly windstorms that , which induced that induced sustained heat loss, surface cooling, and densification of surface waters over the es in the GoL, promoting shallow cascading into the Cap de Creus Canyon.

E. In contrast, easterly and southeasterly winds dominated during the second part of the winter (February and March), and further enhanced shallow cascading into the canyon, the export of dense shelf waters to the southwestern end of the gulf, where they cascaded into the upper section of the Cap de Creus Canyon, region, enhancing the formation of dense shelf waters. Nevertheless, the moderate freshwater inputs from the Rhône River and the smaller coastal rivers decreased the density of shelf waters and, consequently, limited their export into deeper sections of Lacaze Duthiers and Cap de Creus Canyons. In In

In-early March 2022, dense shelf waters were observed at the continental shelf during the in the glider transect survey. These waters cascaded conducted at the continental shelf adjacent to the into the upper canyon down to ~400390 m depth, Cap de Creus Canyon. They were transported to the upper canyon section to depths of ~350 m, where they contributed to the formation of the WIW body. Increased SPM concentrations were also observed were observed associated with these dense shelf waters, at the same water depths, likely indicative of a resuspension process. River discharges were low before and during the FARDWO-CCC1 cruise and, therefore, they were not the main source of suspended sediments during the downwelling phase. Instead, storm-inducedwaves and cascading-induced currents associated Erosion induced by the action of storm waves or strong currents by with cascading waters were likely resuspended and transported the main contributor of suspended sediments SPM associated with the dense water vein transported through the canyon. We estimated an export of roughly dense water of ~0.3 Sv and 10<sup>5</sup> metric tons of sediments on in the upper canyon section. Late winter was marked by persistent northerly and northwesterly windstorms alternated with easterly southeasterly wind events, which reinforced the presence and flushing of dense shelf waters into the Cap de Creus Canyon.

Reanalysis data showed that the cascading season in 2021-2022 provided additional temporal context, revealing that the cascading season period-lasted approximately two three-months (r-from late January to early-mid-March April 2022), with several shallow cascading pulses. Peak transport occurred research is data also showed multiple several shallow cascading events pulses during this period, with the peak export in late January and in mid-March associated with an easterly/southeasterly storm that enhanced shallow cascading likely pushed into dense shelf waters to the canyon. The total dense water transport over the season was ~20ver the entire cascading period, we estimated a total dense shelf water export of ~260 km³. In terms of This volume, the 2021-2022 export was higher than during the mild winters of 1998-1999 and 2003-2004, but lower than in the mild winter of 2010-2011, highlighting the significant variability of MDSWC even under similar mild atmospheric conditions, approximately half of that estimated for the mild winter of 1998-1999 and higher than the export simulated for the mild winter of 2003-2004. Compared towith the extreme winter of 2004-2005, it the 2021-2022 transport represented roughly half of the total dense water volume exported transported, further highlighting the variable nature of DSWC in the region. These contrasts show the episodic and variable nature of DSWC in the GoL. Heat loss seem to be the main factor controlling the density gained by shelf waters during winter, thus the magnitude of the transports. Nevertheless, the exact atmospheric mechanisms driving both MDSWC and IDSWC still deserve further investigation.

Comparison with past events indicates that mild winters can sometimes generate dense water transports comparable in magnitude to those of extreme winters, but the preferential pathways differ. During mild winters, most dense waters flow along the coast or generate shallow cascading to the upper canyon, while in extreme winters, they cascade deep into the canyon and deep basin. Moreover, iIt is likely that, during the winter of 2021-2022, a high proportion of dense waters and associated SPM was exported, highlighting the episodic nature of DSWC. This data also showed that much of the dense water export took place transported along the coast or generated only shallow cascading into the canyon, resembling the export patterns of previously reported MDSWC events., while only a small portion downwelled into the westernmost canyons incising the GoL (namely Lacaze Duthiers and Cap de Creus canyons) between 200 and 400 m depth.

Future investigations—research should further investigate benefit from a more detailed exploration of the physical dynamics driving of MDSWC events. —More importantly, in the context of given the climate change scenario, future studies should focus on the evolution and aim to expand observational datasets, not only within the westernmost canyons incising the gulf but also across the shelf areas. Increasing glider surveys on the GoL's shelf area could improve our understanding of dense water export during weak cascading events under mild winter conditions. Further investigations should also focus on the changes in on the WIW. These studies would help to understand the alterations in the water column properties, and changes in stratification and convection—affecting convection processes, and ultimately which directly impact the impacts on the Mediterranean thermohaline circulation and the functioning of marine the climate systemecosystems.

#### Data availability

. 

The data that support the findings of this study are publicly available under the following links: SeaExplorer glider from (https://data-selection.odatis-ocean.fr/coriolis/uri/p83112098), CCC-1000 moored time series (https://doi.org/10.17882/104746; Sanchez-Vidal et al., 2025a), LDC-500 and LDC-1000 moored time series (https://doi.org/10.17882/45980; Durrieu de Madron et al., 2024). The CTD and the ADCP data collected during the FARDWO-CCC1 Cruise are available at https://doi.org/10.17882/105499 (Sanchez-Vidal et al., 2025b).

#### **Authors contributions**

AS, DA, XD, and FB defined the research problem, the conceptualization of the study, and leaded the acquisition of the study data. MA-C carried out the data analysis and produced the figures and first draft of the manuscript. All coauthors discussed the analyses and contributed to the review and writing of the final paper.

#### **Competing interests**

960

961

962

969

976

977

978

979

980

981

982

983

984

985

986

987

988

989

990

991

992

993

994

995

The authors declare that they have no conflict of interest.

# Acknowledgements

- 963 We are very grateful to the captain, crew, and the scientific team for their dedication and hard work during the FARDWO-
- 964 CCC1 Cruise at the R/V García del Cid, and to the technicians for their guidance and assistance. We wish to thank the Alseamar
- 965 Alcen technicians for the glider deployment and piloting, and the data pre-processing. We also want to thank Pascal Conan
- 966 from OSU-Stamar (Stations Marines UPMC de Banyuls-sur-Mer) at the Sorbonne Université, as well as acknowledge the
- 967 MOOSE, the COAST-HF and the SOMLIT programs coordinated by CNRS-INSU and the Research Infrastructure ILICO
- 968 (CNRS-IFREMER) for providing data from the POEM and SOLA buoys and the Lacaze-Duthiers Canyon's mooring.

#### Financial support

- 970 This work has been supported by the FARDWO (PID2020-114322RB-I00) project funded by
- 971 MICIU/AEI/10.13039/501100011033, the Catalan Government Excellent Research Groups gran no. 2021 SGR 01195, and the
- ANR MELANGE (ANR-19-ASMA-0004) project. MAC was supported by a Margarita Salas postdoctoral grant (2022-2024)
- from the Spanish Ministry of Universities throughout part of the project. ASV acknowledges support from the ICREA program,
- 974 and HF is supported by the AGAUR FI-SDUR fellowship number 2023-FISDU-00233 by Secretaria d'Universitats i Recerca
- 975 from the Catalan Government.

#### References

- Allen, S. E., and Durrieu de Madron, X.: A review of the role of submarine canyons in deep-ocean exchange with the shelf. Ocean Sci. 5, 607-620, https://doi.org/10.5194/os-5-607-2009, 2009.
- Amblas, D., Dowdeswell, J. A.: Physiographic influences on dense shelf-water cascading down the Antarctic continental slope. Earth-Sci. Rev. 185, 887-900, <a href="https://doi.org/10.1016/j.earscirev.2018.07.014">https://doi.org/10.1016/j.earscirev.2018.07.014</a>, 2018.
- Arjona-Camas, M., Puig, P., Palanques, A., Durán, R., White, M., Paradis, S., and Emelianov, M.: Natural vs. trawling-induced water turbidity and suspended sediment transport variability within the Palamós Canyon (NW Mediterranean). Mar. Geophys. Res. 42, 38, https://doi.org/10.1007/s11001-021-09457-7, 2021.
- Béthoux, J., Durrieu de Madron, X., Nyffeler, F., and Taiiliez, D.: Deep water in the western Mediterranean: peculiar 1999 and 2000 characteristics, shelf formation hypothesis, variability since 1970 and geochemical interferences. J. Mar. Sys. 33, 117-131, http://doi.org/ 10.1016/S0924-7963(02)00055-6, 2002.
- Blair, N. E., and Aller, R. C.: The fate of terrestrial organic carbon in the marine environment. Annu. Rev. Mar. Sci. 4, 401-423, https://doi.org/10.1146/annurev-marine-120709-142717, 2012.
- Bourrin, F. and Durrieu de Madron, X.: Contribution to the study of coastal rivers and associated prodeltas to sediment supply in the Gulf of Lions (NW Mediterranean Sea). Life Environ. 56, 307-31, 2006.
- Bourrin, F., Durrieu de Madron, X., Heussner, S., and Estournel, C.: Impact of winter dense water formation on shelf sediment erosion (evidence from the Gulf of Lions, NW Mediterranean). Cont. Shelf Res. 28, 1984-1999, https://doi.org/10.1016/j.csr.2008.06.006, 2008.
- Bourrin, F., Zudaire, L., Vala, T., Vuillemin, R., Conan, P., and Kunesch, S.: POEM Coastal Buoy. SEANOE. https://doi.org/10.17882/88936, 2022.
- Canals, M., Puig, P., Durrieu de Madron, X., Heussner, S., Palanques, A., and Fabres, J.: Flushing submarine canyons.

  Nature 444, 354-357, https://doi.org/10.1038/nature05271, 2006.

1001

1002

**1**003

1004

a rotating fluid. J. Phys. Oceanogr. 34, 188-203, https://doi.org/10.1175/1520 0485(2004)034%3C0188:ADCFDA%3E2.0.CO;2, 2004.

Chapron, L., Lebris, N., Durrieu de Madron, X., Peru, E., Galand, P., and Lartaud, F.: Long term monitoring of coldwater coral growth shows response to episodic meteorological events in the NW Mediterranean. Deep Sea Res. I Oceanogr. Pap. 160, 103255, https://doi.org/10.1016/j.dsr.2020.103255, 2020.

Cenedese, C., Whitehead, J. A., Ascarelli, T. A., and Ohiwa, M.: A dense water current flowing down a sloping

Conan, P., Maria, E., Labatut, P., Zudaire, L., Pujo-Pay, M., Pecqueur, D., Salmeron, C., Crispi, O., Marie, B., and Vuillemin, R.: SOMLIT-SOLA time series (French Research Infrastructure ILICO): long-term core parameter monitoring in the Bay of Banyuls-sur-Mer. SEANOE. https://doi.org/10.17882/99794, 2024.

Danovaro, R., Gambi, C., Dell'Anno, A., Corinaldesi, C., Fraschetti, S., Vanreusel, A., Vincx, M., and Gooday, A.: Exponential decline of deep-sea ecosystem functioning linked to benthic ecosystem loss. Curr. Biol. 18, 1-18, https://doi.org/10.1016/j.cub.2007.11.056, 2008.

Davies, P. A., Dakin, J. M., and Falconer, R. A.: Eddy formation behind a coastal headland. J. Coast. Res. 1, 154-167, http://www.jstor.org/stable/4298318, 1995.

Davis, R. A., and Hayes, M. O.: What is a wave-dominated coast? Mar. Geol. 60, 313-319, https://doi.org/10.1016/0025-3227(84)90155-5, 1984.

DeGeest, A.L., Mullenbach, B. L., Puig, P., Nittrouer, C. A., Drexler, T. M., Durrieu de Madron, X., Orange, D. L.: Sediment accumulation in the western Gulf of Lions, France: the role of Cap de Creus Canyon in linking shelf and slope sediment dispersal systems. Cont. Shelf Res. 28, 2031-2047, https://doi.org/10.1016/j.csr.2008.02.008, 2008.

Dipper, F.: The seawater environment and ecological adaptations, in: Elements of Marine Ecology (Fifth Edition), edited by: Butterworth-Heinemann, Oxford, UK, 37-151, https://doi.org/10.1016/B978-0-08-102826-1.00002-8, 2022.

Drexler, T. M., and Nittrouer, C. A.: Stratigraphic signatures due to flood deposition near the Rhône River: Gulf of Lions, northwest Mediterranean Sea. Cont. Shelf Res. 28, 1877-1894, https://doi.org/10.1016/j.csr.2007.11.012, 2008.

Dufau-Julliand, C., Marsaleix, P., Petrenko, A., and Dekeyser, I.: Three-dimensional modeling of the Gulf of Lion's hydrodynamics (northwest Mediterranean) during January 1999 (MOOGLI3 Experiment) and late winter 1999: Western Mediterranean Intermediate Water's (WIW's) formation and its cascading over the shelf break. J. Geophys. Res. Oceans, 109, https://doi.org/10.1029/2003JC002019, 2004.

Durán, R., Canals, M., Sanz, J. L., Lastras, G., Amblas, D., and Micallef, A.: Morphology and sediment dynamics of the northern Catalan continental shelf, northwestern Mediterranean Sea. Geomorphology, 204, 1-20, https://doi.org/10.1016/j.geomorph.2012.10.004, 2014.

Durrieu de Madron, X., Nyffeler, F., and Godet, C. H.: Hydrographic structure and nepheloid spatial distribution in the Gulf of Lions continental margin. Cont. Shelf Res. 10, 915-929, https://doi.org/10.1016/0278-4343(90)90067-V, 1990.

Durrieu de Madron, X. and Panouse, M.: Transport de matière en suspension sur le plateau continental du Golfe de Lion-Situation estivale et hivernale. Comptes Rendus de l'Académie des Sciences, Série Ila, Paris, 322, 1061-1070, 1996.

Durrieu de Madron, X., Zervakis, V., Therocharis, A., and Georgopoulos, D.: Comments on "Cascades of dense water around the world ocean". Prog. Oceanogr. 64, 83-90, https://doi.org/10.1016/j.pocean.2004.08.004, 2005.

Durrieu de Madron, X., Wiberg, P. L., and Puig, P. Sediment dynamics in the Gulf of Lions: The impact of extreme events. Cont. Shelf Res. 28, 1867-1876, https://doi.org/10.1016/j.csr.2008.08.001, 2008.

Durrieu de Madron, X., Houpert, L., Puig, P., Sanchez-Vidal, A., Testor, P., Bosse, A., Estournel, C., Somot, S., Bourrin, F., Bouin, M. N., Beauverger, M., Beguery, L., Canals, M., Cassou, C., Coppola, L., Dausse, F., D'Ortenzio, F., Font, J., Heussner, S., Kunesch, S., Lefevre, D., Le Goff, H., Martín, J., Mortier, L., Palanques, A., and Raimbault, P.: Interaction of dense shelf water cascading and open-sea convection in the northwestern Mediterranean during winter 2012. Geophys. Res. Lett. 40, 1379-1385, https://doi.org/10.1002/grl.50331, 2013.

1005 1006 1007

1008 1009

1010

1011 1012

1014 1015

1013

1017 1018

1016

1019 1020

1021 1022 1023

1025 1026

1024

1027 1028

1030 1031

1029

1032 1033

1034 1035

1036 1037

1038 1039

- Durrieu de Madron, X., Aubert, D., Charrière, B., Kunesch, S., Menniti, C., Radakovitch, O., and Sola, J.: Impact of dense water formation on the transfer of particles and trace metals from the coast to the deep in the northwestern Mediterranean.

  Water, 15, 301, https://doi.org/10.3390/w15020301, 2023.
- Durrieu de Madron, X., Heussner, S., Delsaut, N., Stéphane, K., Menniti, C.: BILLION observatory data. SEANOE.

  https://doi.org/10.17882/45980, 2024.

1047

1048

1049

1050

10511052

1053

1054

1055

1056

1057

1058

1059

1060

1061

1062

1063

1064

1065

1066

1067

1068

1069

1070

1071

1072

1073

1074

1075

1076

1077

1078

1079

1080

- Escudier, R., Clementi, E., Omar, M., Cipollone, A., Pistoia, J., Aydogdu, A., Drudi, M., Grandi, A., Lyubartsev, V., Lecci, R., Cretí, S., Masina, S., Coppini, G., and Pinardi, N.: Mediterranean Sea Physical Reanalysis (CMEMS MED-Currents) (Version 1) [Data set]. Copernicus Monitoring Environment Marine Service (CMEMS), https://doi.org/10.25423/CMCC/MEDSEA MULTIYEAR PHY 006 004 E3R1, 2020.
- Escudier, R., Clementi, E., Cipollone, A., Pistoia, J., Drudi, M., Grandi, A., Luybartsev, V., Lecci, R., Aydogdu, A., Delrosso, D., Omar, M., Masina, S., Coppini, G., and Pinardi, N.: A high resolution reanalysis for the Mediterranean Sea. Front. Earth Sci. 9, 702285, https://doi.org/10.3389/feart.2021.702285, 2021.
  - Estournel, C., Mikolajczak, G., Ulses, C., Bourrin, F., Canals, M., Charmasson, S., Doxaran, D., Duhaut, T., Durrieu de Madron, D., Marsaleix, P., Palanques, A., Puig, P., Radakovitch, O., Sanchez-Vidal, A., and Verney, R.: Sediment dynamics in the Gulf of Lion (NW Mediterranean Sea) during two autumn–winter periods with contrasting meteorological conditions. Prog. Oceanogr. 210, 102942, https://doi.org/10.1016/j.pocean.2022.102942, 2023.
  - Fabres, J., Tesi, T., Velez, J., Batista, F., Lee, C., Calafat, A., Heussner, S., Palanques, A., and Miserocchi, S.: Seasonal and event-controlled export of organic matter from the shelf towards the Gulf of Lions continental slope. Cont. Shelf Res. 28, 1971-1983, https://doi.org/10.1016/j.csr.2008.04.010, 2008.
  - Ferré, B., Durrieu de Madron, X., Estournel, C., Ulses, C., and Le Corre, G.: Impact of natural (waves and currents) and anthropogenic (trawl) resuspension on the export of particulate matter to the open ocean: application to the Gulf of Lion (NW Mediterranean). Cont. Shelf Res. 28, 2071-2091, https://doi.org/10.1016/j.csr.2008.02.002, 2008.
- Fischer, J., and Visbeck, M.: Deep Velocity Profiling with Self-contained ADCPs. J. Atmos. Ocean. Technol. 10, 764-773, https://doi.org/10.1175/1520-0426(1993)010%3C0764:DVPWSC%3E2.0.CO;2, 1993.
- Font, J.: The path of the Levantine intermediate water to the Alboran Sea. Deep Sea Res. I Oceanogr. Res. Pap. 34, 1745-1755, https://doi.org/10.1016/0198-0149(87)90022-7, 1987.
- Font, J., Puig, P., Salat, J., Palanques, A., and Emelianov, M.: Sequence of hydrographic changes in the NW 2005. Mediterranean deep water due to the exceptional winter of Sci. Mar. 71, 339-346, https://doi.org/10.3989/scimar.2007.71n2339, 2007.
- Fos, H., Izquierdo-Peña, J., Amblas, D., Arjona-Camas, M., Romero, L., Estella-Pérez, V., Florindo-Lopez, C., Calafat, A., Cerdà-Domènech, M., Puig, P., Durrieu de Madron, X., and Sanchez-Vidal, A.: Solving dense shelf water cascading with a high-resolution ocean reanalysis. ESS Open Archive, March 17, https://doi.org/10.22541/essoar.174060515.57729804/v2, 2025.
- Fugate, D.C., and Friedrichs, C.T.: Determining concentration and fall velocity of estuarine particle populations using ADV, OBS and LISST. Cont. Shelf Res. 22 (11–13), 1867–1886, https://doi.org/10.1016/S0278-4343(02)00043-2, 2002.
- Gales, J., Rebesco, M., De Santis, L., Bergamasco, A., Colleoni, F., Kim S., Accetella, A., Kovacevic, V., Liu, Y., Olivo, E., Colizza, E., Florindo-Lopez, C., Zgur, F., McKay, R.: Role of dense shelf water in the development of Antarctic submarine canyon morphology. Geomorphology, 372, 107453, <a href="https://doi.org/10.1016/j.geomorph.2020.107453">https://doi.org/10.1016/j.geomorph.2020.107453</a>, 2021.
- Gartner, J. W.: Estimating suspended soils concentrations from backscatter intensity measured by acoustic Doppler current profiler in San Francisco Bay, California. Mar. Geol. 211, 169-187, https://doi.org/10.1016/j.margeo.2004.07.001, 2004.

Guillén, J., Bourrin, F., Palanques, A., Durrieu de Madron, X., Puig, P., and Buscail, R.: Sediment dynamics during 'wet' and 'dry' storm events on the Têt inner shelf (SW Gulf of Lions). Mar. Geol. 234, 129 142, https://doi.org/10.1016/j.margeo.2006.09.018, 2006.

Guizien, H.: Spatial variability of wave conditions in the Gulf of Lions (NW Mediterranean Sea). Vie et Milieu/Life & Environment, 261-270, 2009.

Herrmann, M., Estournel, C., Déqué, M., Marsaleix, P., Sevault, F., and Somot, S.: Dense water formation in the Gulf of Lions shelf: Impact of atmospheric interannual variability and climate change. Cont. Shelf Res. 28, 2092-2112, https://doi.org/10.1016/j.csr.2008.03.003, 2008.

Hersbach, H., Bell, B., Berrisford, P., Biavati, G., Horányi, A., Muñoz Sabater, J., Nicolas, J., Peubey, C., Radu, R., Rozum, I., Schepers, D., Simmons, A., Soci, C., Dee, D., and Thépaut, J-N. ERA5 hourly data on pressure levels from 1940 to present. Copernicus Climate Change Service (C3S) Climate Data Store (CDS). https://doi.org/10.24381/cds.bd0915c6, 2023.

 Heussner, S., Durrieu de Madron, X., Calafat, A., Canals, M., Carbonne, J., Desault, N., and Saragoni, G.: Spatial and temporal variability of downward particle fluxes on a continental slope: lessons from an 8-yr experiment in the Gulf of Lions (NW Mediterranean). Mar. Geol. 234, 63-92, https://doi.org/10.1016/j.margeo.2006.09.003, 2006.

Homrani, S., de Fommervault, P., Gentil, M., Jourdin, F., Durrieu de Madron, X., Bourrin, F.: Tracing suspended sediment fluxes using a glider: observations in a tidal shelf environment. EGUsphere, 1-35, https://doi.org/10.5194/egusphere-2024-4072, 2025.

Houpert, L., Durrieu de Madron, X., Testor, P., Bosse, A., D'Ortenzio, F., Bouin, M. N., Dausse, D., Le Goff, H., Kunesch, S., Labaste, M., Coppola, L., Mortier, L., and Raimbault, P.: Observations of open-ocean deep convection in the northwestern Mediterranean Sea: Seasonal and interannual variability of mixing and deep water masses for the 2007-2013 Period. J. Geophys. Res. Oceans, 121, 8139-8171, https://doi.org/10.1002/2016JC011857, 2016.

Ivanov, V. V., Shapiro, G. I., Huthnance, J. M., Aleynik, D. L., and Golovin, P. N.: Cascades of dense water around the world. Progr. Oceanogr. 60, 47-98. <a href="https://doi.org/10.1016/j.pocean.2003.12.002">https://doi.org/10.1016/j.pocean.2003.12.002</a>, 2004.

Kwon, E., DeVries, T., Galbraith, E. D., Hwang, J., Kim, G., and Timmermann, A.: Stable carbon isotopes suggest large terrestrial carbon inputs to the global ocean. Global Biogeochem. Cycles 35: e2020GB006684, https://doi.org/10.1029/2020GB006684, 2021.

Juza, M., Renault, L., Ruiz, S., and Tintoré, J.: Origin and pathways of Winter Intermediate Water in the Northwestern Mediterranean Sea using observations and numerical simulation. J. Geophys. Res. 118, 6621-6633, https://doi.org/10.1002/2013JC009231, 2013.

Juza, M., Escudier, R., Vargas-Yáñwz, M., Mourre, B., Heslop, E., Allen, J., and Tintoré, J.: Characterization of changes in Western Intermediate Water properties enabled by an innovative geometry-based detection approach. J. Mar. Sys. 191, 1-12, https://doi.org/10.1016/j.imarsys.2018.11.003, 2019.

Lastras, G., Canals, M., Urgeles, R., Amblas, D., Ivanov, M., Droz, L., Dennielou, B., Fabrés, J., Schoolmeester, T., Akhmetzhanov, A., Orange, D., and García-García, A.: A walk down the Cap de Creus Canyon, Northwestern Mediterranean Sea: Recent processes inferred from morphology and sediment bedforms. Mar. Geol. 246, 176-192, https://doi.org/10.1016/j.margeo.2007.09.002, 2007.

Lapouyade A. and Durrieu de Madron, X.: Seasonal variability of the advective transport of particulate and organic carbon in the Gulf of Lion (NW Mediterranean). Oceanol. Acta, 24, 295-312, https://doi.org/10.1016/S0399-1784(01)01148-3, 2001.

Le Bot, P., Kermabon, C., Lherminier, P., and Gaillard, F.: CASCADE V6.1: Logiciel de validation et de visualisation des mesures ADCP de coque. Rapport technique OPS/LPO 11-01. Ifremer, Centre de Brest, France, 2011.

- Leredde, Y., Denamiel, C., Brambilla, E., Lauer-Leredde, C., Bouchette, F., and Marsaleix, P.: Hydodynamics in the Gulf of Aigues-Mortes, NW Mediterranean Sea: In situ and modelling data. Cont. Shelf Res. 27, 2389-2406, https://doi.org/10.1016/j.csr.2007.06.006, 2007.
- Levin, L. A. and Sibuet, M.: Understanding continental margin biodiversity: a new imperative. Annu. Rev. Mar. Sci. 4, 79-112, http://doi.org/10.1146/annurev-marine-120709-142714, 2012.
- Liu, Z., Zhao, Y., Colin, C., Stattegger, K., Wiesner, M. G., Huh, C. A., Zhang, Y., Li, X., Sompongchaiyakul, P., You, C. F., Huany, C., Liu, J. T., Siringan, F. P., Le, Sathiamurthy, E., Hantoro, W. S., Liu, J., Tuo, S., Zhao, S., Zhou, S., He, Z., Wang, Y., Bunsomboonsakul, S., and Li, Y.: Source-to-sink transport processes of fluvial sediments in the South China Sea. Earth Sci. Rev. 153, 238-273, https://doi.org/10.1016/j.earscirev.2015.08.005, 2016.

11341135

1136

1137

1138

1139

1140

11411142

1143

1144

1145

1146

1147

1148

1149

1150 1151

1152

1153

1154

1155

1156

1157

1158 1159

1160

1161

11621163

- Lohrmann, A.: Monitoring Sediment Concentration with Acoustic Backscattering Instruments. Nortek, 2001.
- Ludwig, W., Dumont, E., Meybeck, M., and Heussner, S.: River discharges of water and nutrients to the Mediterranean and Black Sea: major drivers for ecosystem changes during past and future decades? Prog. Oceanogr. 80, 199-217, https://doi.org/10.1016/j.pocean.2009.02.001, 2009.
- Mack, S. A., and Schoeberlein, H. C.: Richardson number and ocean mixing: towed chain observations. J. Phys. Oceanogr. 34, 736-754, https://doi.org/10.1175/1520-0485(2004)034<0736:RNAOMT>2.0.CO;2, 2004.
- Mahjabin, T., Pattiaratchi, C., Hetzel, Y., and Janekovic, I.: Spatial and temporal variability of dense shelf water cascades along the Rottnest continental shelf in southwest Australia. J. Mar. Sci. Eng. 7, 30, <a href="https://doi.org/10.3390/jmse7020030">https://doi.org/10.3390/jmse7020030</a>, 2019.
- Mahjabin, T., Pattiaratchi, C., and Hetzel, Y.: Occurrence and seasonal variability of Dense Shelf Water Cascades along Australian continental shelves. Sci. Rep. 10, 9732, https://doi.org/10.1038/s41598-020-66711-5, 2020.
- Margirier, F., Testor, P., Heslop, E., Mallil, K., Bosse, A., Houpert, L., Mortier, L., Bouin, M., Coppola, L., D'Ortenzio, F., Durrieu de Madron, X., Mourre, B., Prieur, L., Raimbault, P., and Taillandier, V.: Abrupt warming and salinification of intermediate waters interplays with decline of deep convection in the Northwestern Mediterranean Sea. Sci. Rep. 10, 20923, https://doi.org/10.1038/s41598-020-77859-5, 2020.
- Martín, J., Palanques, A., and Puig, P.: Composition and variability of downward particulate matter in the Palamós submarine canyon (NW Mediterranean). J. Mar. Sys. 60, 75-97, https://doi.org/10.1016/j.jmarsys.2005.09.010, 2006.
- Martín, J., Palanques, A., Puig, P.: Near-bottom horizontal transfer of particulate matter in the Palamós submarine Canyon (NW Mediterranean). J. Mar. Res. 65, 193-218, https://doi.org/10.1357/002224007780882569, 2007.
- Martín, J., Durrieu de Madron, X., Puig, P., Bourrin, F., Palanques, A., Houpert, L., Higueras, M., Sánchez-Vidal, A., Calafat, A. M., Canals, M., Heussner, S., Delsaut, N., and Sotin, C.: Sediment transport along the Cap de Creus canyon flank during a mild, wet winter. Biogeosciences 10(5):3221-3239, https://doi.org/10.5194/bg-10-3221-2013, 2013.
- Marshall, J., and Schott, F.: Open-ocean convection: Observations, theory, and models. Rev. Geophys. 37, 1-64, https://doi.org/10.1029/98RG02739, 1999.
- Mendoza, E. T. and Jiménez, A. A.: Vulnerability assessment to coastal storms at a regional scale. In: Coastal engineering 2008, vol. 5, pp. 4154–4166, https://doi.org/10.1142/9789814277426\_0345, 2009.
- Mikolajczak, G., Estournel, C., Ulses, C., Marsaleix, P., Bourrin, F., Martín, J., Pairaud, I., Puig, P., Leredde, Y., Many, G., Seyfried, L., and Durrieu de Madron, X.: Impact of storms on residence times and export of coastal waters during a mild autumn/winter period in the Gulf of Lion. Cont. Shelf Res. 207, 104192, https://doi.org/10.1016/j.csr.2020.104192, 2020.
- Millot, C.: The Gulf of Lions' hydrodynamics. Cont. Shelf Res. 10, 885-894, https://doi.org/10.1016/0278-4343(90)90065-T, 1990.
- Millot, C.: Circulation in the Western Mediterranean. J. Mar. Syst. 20, 423-442, https://doi.org/10.1016/S0924-7963(98)00078-5, 1999.

1173

1174

1175

11761177

1178

1179

1180

1181

1182

1183

1184

1185

1186

1187

1188

11891190

1191

1192

1193

1194

1195

1196 1197

1198

1199

1200

1201 1202

1203

1204

1205

1206

1207

1208

1169 Nittrouer, C. A., Austin, J. A., Field, M. E., Kravitz, J. H., Syvitski, J. P., and Wiberg, P. L.: Continental margin 1170 sediment to sequence stratigraphy, John Wiley and Sons sedimentation: transport (Eds), 1171 http://doi.org/10.1002/9781444304398, 2009.

Odic, R., Bensoussan, N., Pinazo, C., Taupier-Letage, I., and Rossi, V.: Sporadic wind-driven upwelling/downwelling and associated cooling/warming along Northwestern Mediterranean coastlines. Cont. Shelf Res. 250, 104843, https://doi.org/10.1016/j.csr.2022.104843, 2022.

Ogston, A. S., Drexler, T. M., and Puig, P.: Sediment delivery, resuspension, and transport in two contrasting canyon environments in the southwest Gulf of Lions. Cont. Shelf Res. 28, 2000-2016, https://doi.org/10.1016/j.csr.2008.02.012, 2008.

Palanques, A., Durrieu de Madron, X., Puig, P., Fabrés, J., Guillén, J., Calafat, A., Canals, M., Heussner, S., and Bonnin, J.: Suspended sediment fluxes in the Gulf of Lions submarine canyons. The role of storms and dense water cascading. Mar. Geol. 234, 43-61, https://doi.org/10.1016/j.margeo.2006.09.002, 2006.

Palanques, A., Guillén, J., Puig, P., and Durrieu de Madron, X.: Storm-driven shelf-to-canyon suspended sediment transport at the southwestern Gulf of Lions. Cont. Shelf Res. 28, 1947-1956, https://doi.org/10.1016/j.csr.2008.03.020, 2008.

Palanques, A., Puig, P., Durrieu de Madron, X., Sanchez-Vidal, A., Pasqual, C., Martín, J., Calafat, A., Heussner, S., and Canals, M.: Sediment transport to the deep canyons and open-slope of the western Gulf of Lions during the 2006 intense cascading and open-sea convection period. Prog. Oceanogr. 106, 1-15, https://doi.org/10.1016/j.pocean.2012.05.002, 2012.

Palanques, A., and Puig, P.: Particle fluxes induced by benthic storms during the 2012 dense shelf water cascading and open sea convection period in the northwestern Mediterranean Basin. Mar. Geol. 406, 119-131, https://doi.org/10.1016/j.margeo.2018.09.010, 2018.

Parras-Berrocal, I. M., Vázquez, R., Cabos, W., Sein, D. V., Álvarez, O., Bruno, M., and Izquierdo, A.: Surface and intermediate water changes triggering the future collapse of deep water formation in the North Western Mediterranean. Geophys. Res. Lett. 49, e2021GL095404, https://doi.org/10.1029/2021GL095404, 2022.

Pasqual, C., Sanchez-Vidal, A., Zúñiga, D., Calafat, A., Canals, M., Durrieu de Madron, X., Puig, P., Palanques, A., and Delsaut, N.: Flux and composition of settling particles across the continental margin of the Gulf of Lion: the role of dense shelf water cascading. Biogeosciences, 7, 217-231, https://doi.org/10.5194/bg-7-217-2010, 2010.

Petrenko, A.: Variability of circulation features in the Gulf of Lion, NW Mediterranean Sea. Importance of inertial currents.

Oceanol. Acta 26: 323 338, https://doi.org/10.1016/S0399 1784(03)00038 0, 2008.

Petrenko, A., Dufau, C., and Estournel, C.: Barotropic eastward currents in the western Gulf of Lion, north-western Mediterranean Sea, during stratified conditions. J. Mar. Syst. 74, 406-428, https://doi.org/10.1016/j.jmarsys.2008.03.004, 2008.

Pont, D., Simonnet, J. P., and Walter, A. V.: Medium-term changes in suspended sediment delivery to the ocean: consequences of catchment heterogeneity and river management (Rhône River, France). Estuar. Coast. Shelf Sci. 54, 1-18, http://doi.org/10.1006/ecss.2001.0829, 2002.

Pörtner, H. O. and Knust, R.: Climate change affects marine fishes through oxygen limitation of thermal tolerance. Science, 315, 95-97, https://doi.org/10.1126/science.1135471, 2007.

Poulier, G., Launay, M., Le Bescond, C., Thollet, F., Coquery, M., and Le Coz, J.: Combining flux monitoring and data reconstruction to establish annual budgets of suspended particulate matter, mercury and PCB in the Rhône River from Lake Geneva to the Mediterranean Sea. Sci. Total Environ. 658, 457-273, https://doi.org/10.1016/j.scitotenv.2018.12.075, 2019.

- Provansal, M., Dufour, S., Sabatier, F., Anthony, E. J., Raccasi, G., and Robresco, S.: The geomorphic evolution and sediment balance of the lower Rhône River (southern France) over the last 130 years: Hydropower dams versus other control factors. Geomorphology, 219, 27-41, <a href="https://doi.org/10.1016/j.geomorph.2014.04.033">https://doi.org/10.1016/j.geomorph.2014.04.033</a>, 2014.
- Puig, P.: Dense shelf water cascading and associated beforms. In: Guillén, J., Acosta, J., Chiocci, F., and Palanques,

  A. (eds). Atlas of Bedforms in the Western Mediterranean. Springer, Cham. <a href="https://doi.org/10.1007/978-3-319-33940-5\_7">https://doi.org/10.1007/978-3-319-33940-5\_7</a>,

  2017.

1216

1217

1218

1219

1220

1221

1222

1223

1224

1225

1226

1227

1228

1229

1233

1234

1235

1236

1237

1238

- Puig, P., Company, J. B., Sardà, F., and Palanques, P.: Responses of deep-water shrimp populations to intermediate nepheloid layer detachments on the Northwestern Mediterranean continental margin. Deep Sea Res. I Oceanogr. Res. Pap. 48, 2195-2207, https://doi.org/10.1016/S0967-0637(01)00016-4, 2001.
- Puig, P., Palanques, A., Orange, D. L., Lastras, G., and Canals, M.: Dense shelf water cascades and sedimentary furrow formation in the Cap de Creus Canyon, northwestern Mediterranean Sea. Cont. Shelf Res. 28, 2017-2030, https://doi.org/10.1016/j.csr.2008.05.002, 2008.
- Puig, P., Palanques, A., and Martín, J.: Contemporary sediment-transport in submarine canyons. Annu. Rev. Mar. Sci. 6, 53-77, https://doi.org/10.1146/annurev-marine-010213-135037, 2014.
- Pusceddu, A., Mea, M., Canals, M., Heussner, S., Durrieu de Madron, X., Sanchez-Vidal, A., Bianchelli, S., Corinaldesi, A., Dell'Anno, A., Thomsen, L., and Danovaro, R.: Major consequences of an intense dense shelf water cascading event on deep-sea benthic trophic conditions and meiofaunal biodiversity. Biogeosciences 10, 2659-2670, https://doi.org/10.5194/bg-10-2659-2013, 2013.
- Ribó, M., Puig, P., Palanques, A., and Lo Iacono, C.: Dense shelf water cascades in the Cap de Creus and Palamós submarine canyons during winters 2007 and 2008. Mar. Geol. 284, 175-188, https://doi.org/10.1016/j.margeo.2011.04.001, 2011.
- Rumín-Caparrós, A., Sanchez-Vidal, A., Calafat, A. M., Canals, M., Martín, J., Puig, P., and Pedrosa-Pàmies, R.:
  External forcings, oceanographic processes and particle flux dynamics in Cap de Creus submarine canyon, NW Mediterranean.
  Biogeosciences Discussions 9(12), https://digital.csic.es/handle/10261/78113, 2013.
  - Sadaoui, M., Ludwig, W., Bourrin, F., and Raimbault, P.: Controls, Budgets and Variability of Riverine Sediment Fluxes to the Gulf of Lions (NW Mediterranean Sea). J. Hydrol. 540, 1002–1015, https://doi.org/10.1016/j.jhydrol.2016.07.012, 2016.
  - Sanchez-Vidal, A., Pasqual, C., Kerhervé, P., Heussner, S., Palanques, A., Durrieu de Madron, X., Canals, M., and Puig, P.: Impact of dense shelf water cascading on the transfer of organic matter to the deep western Mediterranean basin. Geophys. Res. Lett. 35, https://doi.org/10.1029/2007GL032825, 2008.
- Sanchez-Vidal, A., Calafat, A., Amblas, D., Cerdà-Domènech, M., Fos, H.: CC1000 observatory data. SEANOE. https://doi.org/10.17882/105504, 2025a.
- Sanchez-Vidal, A., Amblas, D., Arjona-Camas, M., Durrieu de Madron, X., Calafat, A., Cerdà-Domènech, M., Pena, L.D., Espinosa, S.: CTD and ADCP data collected during the cruise FARDWO CC1. SEANOE. <a href="http://doi.org/10.17882/105499">http://doi.org/10.17882/105499</a>, 2025b.
  - Schlitzer, R.: Ocean Data View. https://odv.awi.de/, 2023.
- Schroeder, K., Josey, S. A., Herrmann, M., Grignon, L., Gasparini, G. P., and Bryden, H. L.: Abrupt warming and salting of the Western Mediterranean Deep Water: Atmospheric forcings and lateral advection. J. Geophys. Res., 115, C08029, https://doi.org/10.1029/2009JC005749, 2010.
- Schroeder, K., Ben Ismail, S., Bensi, M., Bosse, A., Chiggiato, K., Civitarese, G., Falcieri M, F., Fusco, G., Gacic,
- 1249 M., Gertman, I., Kubin, E., Malanotte-Rizzoli, P., Martellucci, R., Menna, M., Ozer, T., Taupier-Letage, I., Vargas-Yañez,
- 1250 M., Velaoras, D. and Vilibic, I.: A consensus-based, revised and comprehensive catalogue for Mediterranean water masses
- acronyms. Mediterranean Marine Science, 25(3), 783–791, https://doi.org/10.12681/mms.38736, 2024.

Serrat, P., Ludwig, W., Navarro, B., and Blazi, J. L.: Variabilité spatio-temporelle des flux de matières en suspension d'un fleuve côtier méditerranéen: la Têt (France). Comptes Rendus de l'Académie des Sciences-Series IIA-Earth and Planetary Science, 333(7), 389-397, https://doi.org/10.1016/S1251-8050(01)01652-4, 2001.

Shapiro, G. I., and Hill, A. E.: The alternative density structures of cold/saltwater pools on a sloping bottom: the role of friction. J. Phys. Oceanogr. 33, 390-406, <a href="https://doi.org/10.1175/1520-0485(2003)033<0390:TADSOC>2.0.CO;2">https://doi.org/10.1175/1520-0485(2003)033<0390:TADSOC>2.0.CO;2</a>, 2003.

Smith, M. D., Knapp, A. K., and Collins, S. L.: A framework for assessing ecosystem dynamics in response to chronic resource alterations induced by global change. Ecology, 90, 3279-3289, https://doi.org/10.1890/08-1815.1, 2009.

Somot, S., Sevault, F., and Déqué, M.: Transient climate change scenario simulation of the Mediterranean Sea for the twenty-first century using a high-resolution ocean circulation model. Clim. Dynam. 27, 851-879, https://doi.org/10.1007/s00382-006-0167-z, 2006.

Somot, S., Houpert, L., Sevault, F., Testor, P., Bosse, A., Taupier-Letage, I., Bouin, M. N., Waldman, R., Cassou, C., Sanchez-Gomez, E., Durrieu de Madron, X., Adloff, F., Nabat, P., and Herrmann, M.: Characterizing, modelling and understanding the climate variability of the deep water formation in the North-Western Mediterranean Sea. Clim. Dynam. 51, 1179-1210, https://doi.org/10.1007/s00382-016-3295-0, 2016.

Taillandier, V., D'Ortenzio, F., Prieur, L., Conan, P., Coppola, L., Cornec, M., Dumas, F., Durrieu de Madron, X., Fach, B., Fourrier, M., Gentil, M., Hayes, D., and Husrevoglu, S.: Sources of the Levantine Intermediate Water in winter 2019. J. Geophys. Res. Oceans, 127, e2021JC017506, https://doi.org/10.1029/2021JC017506, 2022.

Tesi, T., Puig, P., Palanques, A., and Goñi, M.: Lateral advection of organic matter in cascading-dominated submarine canyons. Prog. Oceanogr. 84, 185-203, https://doi.org/10.1016/j.pocean.2009.10.004, 2010.

Testor, P., Bosse, A., Houpert, L., Margirier, F., Mortier, L., Le Goff, H., Dausse, D., Labaste, M., Kartensen, J., Hayes, D., Olita, A., Ribotti, A., Schroeder, K., Chiggiato, J., Onken, R., Heslop, E., Mourre, B., D'Ortenzio, F., Mayot, N., Lavigne, H., Durrieu de Madron, X., Bourrin, F., Many, G., Damien, P., Estournel, C., Marsaleix, P., Taupier-Letage, I., Raimbault, P., Waldman, R., Bouin, M. N., Giordani, H., Caniaux, G., Somot, S., Ducrocq, V., and Conan, P.: Multiscale observations of deep convection in the northwestern Mediterranean Sea during winter 2012-2013 using multiple platforms. J. Geophys. Res. Oceans, 123, 1745-1776, https://doi.org/10.1002/2016JC012671, 2018.

Thurnherr, A. M.: A practical assessment of the errors associated with full-depth LADCP profiles obtained using Teledyne RDI Workhorse acoustic Doppler current profilers. J. Atmos. Oceanic. Technol. 27, 1215-1227, https://doi.org/10.1175/2010JTECHO708.1, 2010.

Thurnherr, A. M., Symonds, D., and Laurent, L. S.: Processing explorer ADCP data collected on slocum gliders using the LADCP shear method. In Proceedings of the 2015 IEEEOES 11<sup>th</sup> Current Waves and Turbulence Measurement CWTM. St. Petersburg, FL, USA 2-6 March 2015, https://doi.org/10.1109/CWTM.2015.7098134, 2015.

Tubau, X., Lastras, G., Canals, M., Micallef, A., and Amblas, D.: Significance of the drainage pattern for submarine canyon evolution: The Foix Canyon System, Northwestern Mediterranean Sea. Geomorphology, 184, 20-37, <a href="https://doi.org/10.1016/j.geomorph.2012.11.007">https://doi.org/10.1016/j.geomorph.2012.11.007</a>, 2013.

Ulses, C., Estournel, C., Bonnin, J., Durrieu de Madron, X., and Marsaleix, P.: Impact of storms and dense water cascading on shelf-slope exchanges in the Gulf of Lion (NW Mediterranean). J. Geophys. Res. Oceans, 113, http://doi.org/10.1029/2006JC003795, 2008a.

Ulses, C., Estournel, C., Puig, P., Durrieu de Madron, X., and Marsaleix, P.: Dense shelf water cascading in the northwestern Mediterranean during the cold winter 2005: Quantification of the export through the Gulf of Lion and the Catalan margin. Geophys. Res. Lett. 35(7), https://doi.org/10.1029/2008GL033257, 2008b.

1293	Visl	beck, M.	: Deep velocit	y profiling usi	ng lowered aco	ustic Dop	pler current pro	ofilers: Bottom track and inverse		
1294	solutions.	J.	Atmos.	Oceanic	Technol.	19,	794-807,	https://doi.org/10.1175/1520-		
1295	0426(2002)019%3C0794:DVPULA%3E2.0.CO;2, 2002.									
1296	Walsh, J. P., and Nittrouer, C. A.: Understanding fine-grained river-sediment dispersal on continental margins. Mar.									
1297	Geol. 263, 34-45, https://doi.org/10.1016/j.margeo.2009.03.016, 2009.									
1298	Wilson, G. W., and Hay, A. E.: Acoustic backscatter inversion for suspended sediment concentration and size: a new									

Wilson, G. W., and Hay, A. E.: Acoustic backscatter inversion for suspended sediment concentration and size: a new approach using statistical inverse theory. Cont. Shelf Res. 106, 130-139, https://doi.org/10.1016/j.csr.2015.07.005, 2015.

Zúñiga, D., Flexas, M. M., Sanchez-Vidal, A., Coenjaerts, J., Calafat, A., Jordà, G., García-Orellana, J., Puigdefàbregas, J., Canals, M., Espino, M., Sardà, M., and Company, J. B.: Particle fluxes dynamics in Blanes submarine canyon (Northwestern Mediterranean). Prog. Oceanogr. 82, 239-251, <a href="https://doi.org/10.1016/j.pocean.2009.07.002">https://doi.org/10.1016/j.pocean.2009.07.002</a>, 2009.

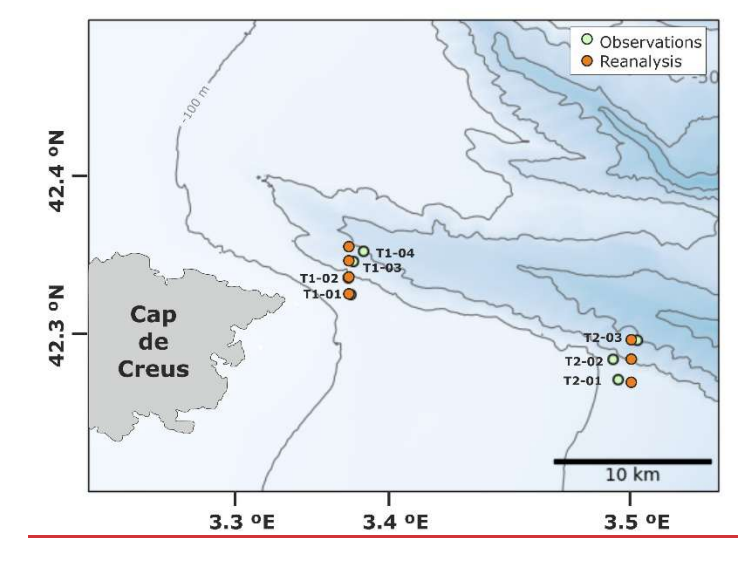
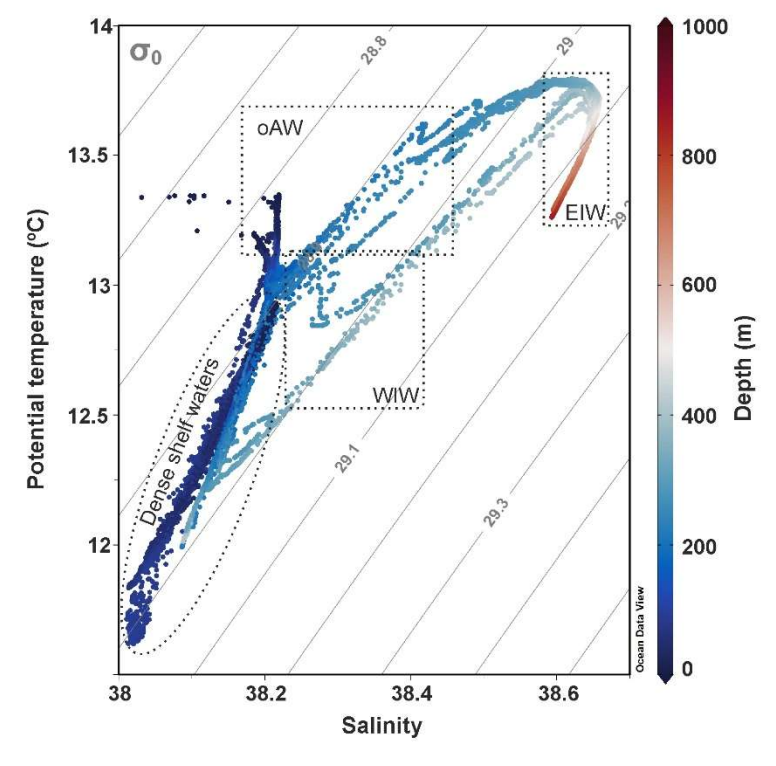


Figure A1. Spatial distribution of CTD stations (green dots) across the Cap de Creus Canyon during the FARDWO-CCC1 cruise where dense shelf waters were observed, and the corresponding MedSea reanalysis grid points (orange dots). Reanalysis data were obtained from the Mediterranean Sea Physics Reanalysis product (Escudier et al., 2020; 2021).



**Figure A1B1.** TS diagram from the CTD profiles collected during FARDWO-CCC1 T1 and T2 transects across the Cap de Creus Canyon, as well as those collected during the glider survey at the adjacent shelf (see Fig. 1b for positions). The different water masses that can be identified in the study area are: dense shelf waters, oAW (old Atlantic Water), WIW (Western Intermediate Water), and EIW (Eastern Intermediate Water).

1326 1\$27

1328

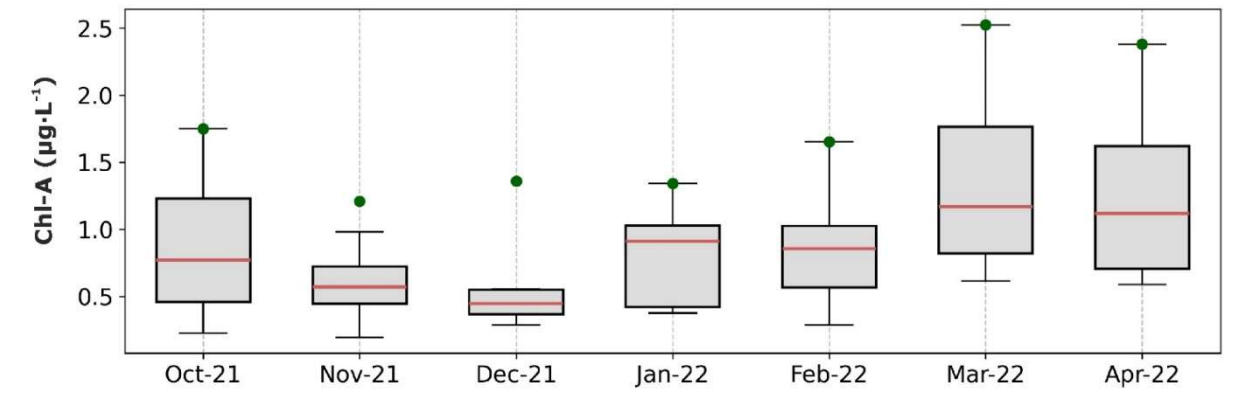


**Figure B1C1.** Seasonality of the chlorophyll-a measured at SOLA station between October 2021 and April 2022. Green dots indicate the monthly maximum values. Data has been retrieved from the SOMLIT-SOLA monitoring site in the Bay of Banyuls-sur-Mer (https://www.seanoe.org/data/00886/99794/; Conan et al., 2024).

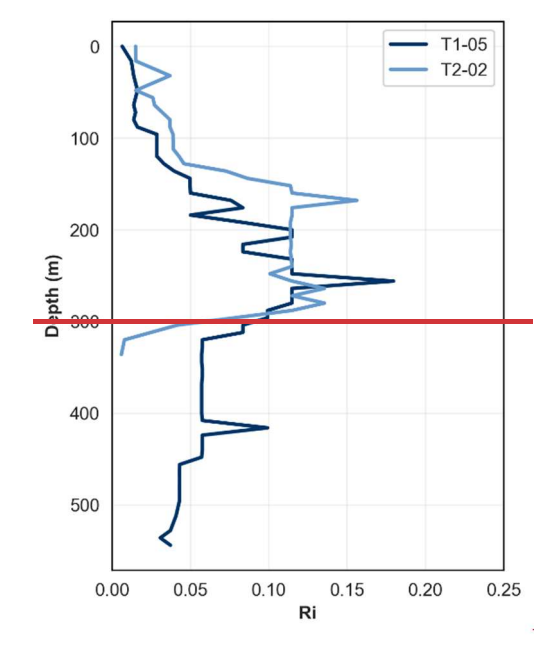


Figure C1. Vertical profiles of the Richardson number (Ri) calculated from CTD and LADCP measurements at two locations at the Cap de Creus Canyon where dense water were observed: T1-05 (upper canyon transect, dark blue) and T2-03 (mideanyon transect, light blue). Values Ri <1 indicate a turbulent regime.